

**The Role of Smooth Muscle Myosin Isoforms
in a Model of Innate Airway Hyperresponsiveness**

F. Roberto Gil

**Department of Physiology
McGill University, Montreal**

May 2006

**A thesis submitted to McGill University in partial fulfillment of the requirements of
the degree of Master of Science**

©Copyright 2006, F. Roberto Gil

All rights reserved.



Library and
Archives Canada

Bibliothèque et
Archives Canada

Published Heritage
Branch

Direction du
Patrimoine de l'édition

395 Wellington Street
Ottawa ON K1A 0N4
Canada

395, rue Wellington
Ottawa ON K1A 0N4
Canada

Your file Votre référence

ISBN: 978-0-494-24677-1

Our file Notre référence

ISBN: 978-0-494-24677-1

NOTICE:

The author has granted a non-exclusive license allowing Library and Archives Canada to reproduce, publish, archive, preserve, conserve, communicate to the public by telecommunication or on the Internet, loan, distribute and sell theses worldwide, for commercial or non-commercial purposes, in microform, paper, electronic and/or any other formats.

The author retains copyright ownership and moral rights in this thesis. Neither the thesis nor substantial extracts from it may be printed or otherwise reproduced without the author's permission.

AVIS:

L'auteur a accordé une licence non exclusive permettant à la Bibliothèque et Archives Canada de reproduire, publier, archiver, sauvegarder, conserver, transmettre au public par télécommunication ou par l'Internet, prêter, distribuer et vendre des thèses partout dans le monde, à des fins commerciales ou autres, sur support microforme, papier, électronique et/ou autres formats.

L'auteur conserve la propriété du droit d'auteur et des droits moraux qui protègent cette thèse. Ni la thèse ni des extraits substantiels de celle-ci ne doivent être imprimés ou autrement reproduits sans son autorisation.

In compliance with the Canadian Privacy Act some supporting forms may have been removed from this thesis.

Conformément à la loi canadienne sur la protection de la vie privée, quelques formulaires secondaires ont été enlevés de cette thèse.

While these forms may be included in the document page count, their removal does not represent any loss of content from the thesis.

Bien que ces formulaires aient inclus dans la pagination, il n'y aura aucun contenu manquant.


Canada

ACKNOWLEDGEMENTS

I would like to particularly thank my supervisor Dr. Anne-Marie Lauzon for countless time advising and guiding me in my project and helping me to challenge my way of thinking. I would like to thank those that have given me considerable help in my Master's thesis, especially Dr. Renaud Leguillette, Dr. Nedjma Zitouni, and Dr. James G. Martin for their help with my project and experiments. I also thank in particular Dr. R.W. Mitchell (University of Chicago) for advice and guidance on our physiology apparatus, Prof. Anders Arner (Lund University, Sweden), Prof. Newman L. Stephens (University of Manitoba), and Prof. Per Hellstrand (Lund University) for discussions and advice, and Dr. Andra Stevenson of Prof. A.V. Somlyo's lab (University of Virginia) for help with the permeabilization protocol. Thanks to the Réseau en Santé Respiratoire, the MUHC-RI, and the Montreal Chest Institute for funding. I would also like to express my gratitude to all the staff of the Meakins-Christie Laboratories, who have made my experience there one of the best.

TABLE OF CONTENTS

ACKNOWLEDGMENTS	ii
TABLE OF CONTENTS	iii
LIST OF TABLES	v
LIST OF FIGURES	vi
ABSTRACT	vii
ABRÉGÉ	viii
CHAPTER I. INTRODUCTION	1
1.1. ASTHMA STATISTICS AND BACKGROUND	1
1.2. AIRWAY HYPERRESPONSIVENESS	3
1.2.1. Inflammation and airway hyperresponsiveness	4
1.2.2. Airway remodeling and the external load on airway smooth muscle	4
1.2.3. Impaired airway relaxation.....	7
1.2.4. Role of airway epithelium	8
1.2.5. Airways smooth muscle plasticity.....	9
1.2.6. Hyperresponsive airway smooth muscle contractility	10
1.3. SMOOTH MUSCLE	12
1.3.1. Introduction.....	12
1.3.2. Smooth muscle types	13
1.3.3. Smooth muscle contractility.....	15
1.4. FISHER & LEWIS RAT MODEL OF AIRWAY HYPERRESPONSIVENESS	26
THESIS RATIONALE AND OBJECTIVES.....	29
CHAPTER II. MATERIALS AND METHODS	31
2.1. MATERIALS.....	31
2.1.1. Animals.....	31
2.1.2. Reagents.....	31
2.2. REAL-TIME QPCR OF (+)INSERT SMMHC ISOFORMS.....	32
2.3. WESTERN BLOT OF CONTRACTILE PROTEIN EXPRESSION.....	34
2.3.1. Tissue preparation.....	34
2.3.2. Western blot of (+)insert and total SMMHC	35
2.3.3. Western blot of actin, caldesmon, and LC ₁₇ isoforms.....	36
2.3.4. List of antibodies	37
2.4. SEQUENCING OF THE HUMAN (+)INSERT SMMHC ISOFORM	38
2.4.1. Identification of the human (+)insert.....	38
2.4.2. Sequencing of the full-length (+)insert isoforms.....	39
2.5. LC ₂₀ PHOSPHORYLATION TO SUB-MAXIMAL STIMULUS IN FISHER AND LEWIS RAT TRACHEAL SMOOTH MUSCLE	40

2.5.1. Trachealis Contractility:	40
2.5.2. LC ₂₀ Phosphorylation Analysis	41
2.6. MUSCLE STRIP MECHANICS AND THIOPHOSPHORYLATION	43
2.6.1. Muscle strip preparation	43
2.6.2. Intact muscle strip measurements.....	44
2.6.3. Muscle permeabilization and thiophosphorylation.....	45
2.7. STATISTICS	48
CHAPTER III. RESULTS	49
3.1. REAL-TIME QPCR EXPRESSION OF (+)INSERT SMMHC ISOFORMS IN FISHER AND LEWIS RATS.....	49
3.2. CONTRACTILE PROTEIN EXPRESSION.....	51
3.3. SEQUENCING THE COMPLETE (+)INSERT SMMHC cDNA	56
3.4. MYOSIN REGULATORY LIGHT CHAIN (LC ₂₀) PHOSPHORYLATION RESPONSE IN FISHER & LEWIS ANIMALS.....	57
3.5. THIOPHOSPHORYLATED FISHER & LEWIS TRACHEAL STRIPS.....	64
3.5.1. Intact muscle strip measurements.....	64
3.5.2. Muscle thiophosphorylation	68
CHAPTER IV. DISCUSSION	71
FINAL CONCLUSION AND SUMMARY	81
REFERENCES	82

LIST OF TABLES

Table 1: Table of reagents used for permeabilized muscle strips (in mM).	47
--	----

LIST OF FIGURES

Figure 1: Smooth muscle myosin.	18
Figure 2: Expression of (+)insert isoform mRNA content in Fisher and Lewis rat smooth muscle.	50
Figure 3: (+)insert isoform and total SMMHC protein content in Fisher and Lewis tracheae.	53
Figure 4: Western blots of other contractile proteins in smooth muscle from Fisher and Lewis ras.	55
Figure 5: Dose-response curve of Fisher and Lewis tracheal smooth muscle strip to MCh.	58
Figure 6: Isometric force response to submaximal stimulus of Fisher and Lewis tracheal strips.	60
Figure 7: LC ₂₀ phosphorylation mounted to submaximal stimulus with MCh in Fisher and Lewis tracheal strips.	63
Figure 8: Representative active length-tension relation of trachealis.	65
Figure 9: Representative force-velocity curves of Fisher and Lewis trachealis.	66
Figure 10: Velocity of maximal shortening for Fisher and Lewis tracheal strips (preliminary).	67
Figure 11: Force development of thiophosphorylated tracheal strips from Fisher and Lewis rats.	70

ABSTRACT

Airway hyperresponsiveness (AHR) is a key feature of asthma, characterized by exaggerated rate and extent of shortening of airway smooth muscle. Two isoforms of the smooth muscle myosin differ by the presence [(+)insert] or absence [(-)insert] of a 7 amino acid insert. The (+)insert exhibits a 2-fold greater ATPase activity and velocity of actin filament propulsion in the *in vitro* motility assay. The expression of these isoforms and other contractile proteins was quantified in the trachea of the Fisher and Lewis rat model of innate AHR. We found 95% greater mRNA and 45% greater protein expression of the (+)insert isoform in the trachea of the hyperresponsive Fisher animal ($p < 0.01$), but no difference in other contractile proteins. A greater extent of myosin phosphorylation was also observed (55.1 ± 6.4 vs. 41.4 ± 6.1 , $p < 0.01$). These results suggest that in addition to greater myosin activation, an increased expression of the (+)insert isoform contribute to AHR.

ABRÉGÉ

L'hyperréactivité bronchique (HB) est un trait important de l'asthme, caractérisé par une vitesse et un raccourcissement exagérés du muscle lisse des voies aériennes. Deux isoformes de la chaîne lourde de la myosine du muscle lisse diffèrent par la présence [(+)insert] ou l'absence [(-)insert] de 7 acides aminés. Le (+)insert possède une ATPase et une vélocité de propulsion de l'actine 2-fois supérieure. L'expression des isoformes de myosine et autres protéines contractiles a été quantifiée chez les rats Fisher et Lewis, un model d'HB innée. Nous avons trouvé une expression du (+)insert 95% supérieure au niveau de l'ARNm et 45% au niveau protéinique dans les trachées hyperréactives des rats Fishers ($p < 0.01$) mais aucune différence pour les autres protéines contractiles. Une plus grande phosphorylation de la chaîne régulatrice a aussi été observée (55.1 ± 6.4 vs. 41.4 ± 6.1 , $p < 0.01$). Ces résultats suggèrent qu'en plus d'une activation élevée, une augmentation de l'expression du (+)insert contribue à l'HB.

CHAPTER I. INTRODUCTION

1.1. ASTHMA STATISTICS AND BACKGROUND

While the mortality rate of asthma in Canada has been slowly declining due to increased public awareness and better healthcare management, it is a disorder of increasing preponderance, affecting more than eight percent of the Canadian population and an estimated 150 million worldwide [19,112]. Considerable progress has been made in determining the origins of asthma, revealing clear contributions from genetic, environmental, and psychological factors. However, a clear understanding and description of its onset, progression, and characteristics continue to remain elusive, and this is largely a consequence of the heterogeneous nature of asthma.

The National Heart, Lung, and Blood Institute has defined asthma as a disorder of the airways characterized by reversible obstruction, hyperresponsiveness, and inflammation [92]. Of these events, the most adverse symptoms of asthma arise from acute narrowing of the airways due to shortening of the airway smooth muscle (ASM) [11,27,101]. Asthmatic airways differ from normal airways in that they are generally responsive to allergens, and more sensitive and more responsive to contractile agonists and other inducers of airway narrowing [31]. The significance of airway hyperresponsiveness is underscored by the fact that it is correlated with the

clinical severity of asthma symptoms [25] and the extent of treatment required for their management [61].

1.2. AIRWAY HYPERRESPONSIVENESS

Airway responsiveness is an index of the extent of airway narrowing that is elicited in response to a contractile stimulus. There is considerable variability in the degree of airway responsiveness among the general population that likely arises from differences in genetic and/or environmental backgrounds [24,120]. Airway responsiveness can also differ depending on the age of the individual. Adolescent individuals characteristically possess a greater degree of airway responsiveness than adults [21], and this likely plays a significant role in determining why asthma affects them more than adults.

Airway hyperresponsiveness is defined as an abnormally exaggerated narrowing response to a given agonist, incorporating some degree of airway hypersensitivity and hyperreactivity to contractile agonists [133]. This phenomenon includes a steeper slope of the dose-response curve for airway response to contractile agonist, and greater extent of maximal airway narrowing [94]. According to Poiseuille's equation, a given change in tube radius will reflect in a change to the fourth power in flow. As such, even small changes in airway diameter by airway smooth muscle shortening can result in dramatic effects on airflow. A number of theories have been proposed to explain the mechanisms by which exaggerated airway narrowing arises in airway hyperresponsiveness, including alterations of the ASM and remodeling of the airways.

1.2.1. Inflammation and airway hyperresponsiveness

A lot of work has gone into addressing how the airway narrowing response in asthmatics differs from normal airways. A number of studies have suggested that the inflammatory response in airways triggers the heightened responsiveness of the airways [37,107]. While a number of studies have shown that inflammation can modify the behavior of ASM [88], work on ASM from asthmatic individuals suggests that their intrinsic contractile properties are also distinct [11,81]. Indeed, while inflammation could exacerbate dyspnea and enhance airway narrowing, it might play only a secondary role in acute episodes of asthma [57].

1.2.2. Airway remodeling and the external load on airway smooth muscle

Airway remodeling is frequently referred to as an epiphenomenon of asthma, likely resulting from inflammation in the airways. Remodeling of the airways includes any of the following: an increased prevalence of fibrotic tissue, increased submucosal mass, and hyperplasia and hypertrophy of the ASM [54,95]. However, the specific characteristics and degree of remodeling that occurs in asthmatic airways is disputed, given the varying degrees of remodeling that have been observed from

asthmatic airways. The extent to which each of these factors affects pulmonary mechanics remains to be investigated. For instance, submucosal thickening of the airways had been predicted to amplify the effect of airway narrowing caused by ASM contraction [70]. An *in vivo* study, however, showed that thicker airways instead narrow to a lesser extent compared to those with thinner walls [93]. The conclusion was made that airway remodeling is not uniform, and that other airways with less or no airway wall thickening are responsible for airflow limitation [10].

Conversely, inflammation has been implicated in causing local connective tissue destruction, thereby reducing the load on the ASM and allowing a faster velocity of contraction [11]. Thus, for a given contractile response of the ASM, a greater change in the caliber of the airways would ensue, and even subthreshold stimuli would be capable of exerting significant effects on airway narrowing. Studies on the significance of inflammation on ASM contractility are underway, although it is also possible that inflammation and abnormal ASM contractility are independent processes that operate in parallel to produce the symptoms of asthma [5].

Whether smooth muscle mass in asthmatic airways is increased is a topic presently under debate. ASM hypertrophy has been described in asthmatic airways [32] and models of airway hyperresponsiveness [35]. However, the only data on ASM hypertrophy in asthma comes from fatal asthma. Given the low availability of such airways, it is unclear if this occurs in milder forms of the disease. Others reported increased ASM contractility with no change in ASM mass in hyperresponsive

airways [52,59], and no evidence for increased ASM mass in asthma [121]. Thomson and coworkers [121] further reported no differences in the extracellular matrix content or the connective tissue content in asthmatic airways, further supporting the significance of hypercontractile ASM in asthma.

The load on the ASM in the smaller airways is thought to be due to a combination of the tethering forces of the parenchyma on the airway, connective tissue fibers within the airway itself, and distortion of the epithelial and submucosal lining during airway narrowing [82,95]. One would therefore expect these factors to play a pivotal role in limiting the extent of airway narrowing, even in asthma. However, a stark difference in the dose-response curves to inhaled bronchoconstrictors has been shown between asthmatic and healthy individuals. Controls individuals will plateau in their airway response after a certain dose, whereas a majority of asthmatics seemingly do not exhibit such a plateau, and rather exhibit a continuing increase in their airway response [134]. Moreover, parenchymal tethering of the airways was suggested to be responsible for the plateau response in the normals, preventing airway closure. This tethering effect would presumably be reduced in asthmatic airways, allowing a greater degree of airway narrowing. However, airway closure was demonstrated in naïve dogs by direct application of contractile agonist [12], suggesting that the underlying ASM has the capacity to overcome the load placed on it to fully close the airways.

1.2.3. Impaired airway relaxation

Another phenomenon supporting the notion that some intrinsic properties of asthmatic ASM are different is that of impaired airway relaxation. The stretching of ASM, as during a deep inspiration (DI), has been suggested to be the most potent of all inducers of airway relaxation [42]. However, it was shown that deep breaths in asthmatic airways do not produce this relaxation response [38], and may even exacerbate symptoms [75]. Upon methacholine challenge, the caliber of a healthy individual's airway will return to normal after a DI. In asthmatics, the airway remains narrowed despite the DI. Interestingly, when normal patients given aerosolized methacholine were directed to avoid taking deep breaths, their airways remained constricted, similar to the asthmatics [105]. Subsequent work on this observation has revealed that this bronchoconstriction in the absence of DI was actually still appreciably greater in asthmatics compared to controls [14,15].

Recently, Brown and colleagues [13] demonstrated that a deep inhalation caused a similar degree of transient bronchodilation in both asthmatic and normal airways following bronchoconstrictive challenge. However, whereas the normal lungs remained bronchodilated following DI, the asthmatic airways in fact had become further bronchoconstricted to levels exceeding those preceding the DI [13]. Further work showed that the time course of the airway re-narrowing following DI was faster in asthmatics [53]. These data suggest that abnormalities in the paren-

chyma likely do not play a major role in the limited beneficial effect of DI in asthma, and instead implicate an abnormality in ASM contractility as orchestrating the rapid airway narrowing that follows a DI in asthma.

1.2.4. Role of airway epithelium

The airway epithelium has also been implicated in airway hyperresponsiveness, as it is well known to influence the contractility and relaxation of the underlying smooth muscle. Airway epithelium is known to produce arachidonic acid-derived factors, nitric oxide, and other mediators which in turn exert either excitatory or inhibitory influences on ASM contractility [39,68,111]. The effect that the epithelium produces on the surrounding smooth muscle is also known to change during development [20], and has been suggested to explain ontogenic differences in ASM contractility [22]. In cases of severe asthma, the airway epithelium can be damaged or completely lost [23,55], and a loss of the regulatory function played by the epithelium could lead to abnormal ASM function. However, much remains to be understood of the relationship between the epithelium and ASM, as epithelial influences on ASM contractility has been shown to have interspecies differences [20].

1.2.5. Airways smooth muscle plasticity

In skeletal and cardiac muscles, it is known that the muscle can sustain a maximum force-generating capacity at a length, and this length is thought to correspond to an optimal alignment of the sarcomeric structures within the muscle to generate force. Plasticity is a phenomenon recently described to explain the process by which smooth muscle appears to defy this well-described property of the striated muscles, wherein maximal force-generating capacity is retained over a range of muscle lengths. This process is putatively accomplished by a parallel to series rearrangement of the thick and thin filaments, or myosin and actin filaments, respectively [97]. These thick and thin filaments that are common to all muscles are known to be particularly labile when it comes to smooth muscle [45,69]. Alternatively, actin filament elongation has been postulated as another mechanism wherein smooth muscle can retain force over a range of lengths, in that it allows for a preservation of the number of contractile elements in parallel over varying muscle lengths. This process has been termed muscle elasticity [31].

With respect to airway hyperresponsiveness, it has been suggested that the number of contractile elements in parallel remains steady in hyperresponsive ASM, such that the elasticity of hyperresponsive ASM is greater than normal [37]. Actin filament length is believed to be regulated by the p38 mitogen activated protein kinase pathway, and is currently the subject of further study [31]. However, while

this phenomenon may occur in airway hyperresponsiveness, it is limited in its explanation for the intrinsically greater rate of muscle shortening that has been well characterized in hyperresponsive ASM, a property that is independent of the number of contractile filaments in parallel. Indeed, velocity of muscle shortening is a property that is closely linked to the ATPase activity of the muscle [59], in turn determined by the intrinsic properties of the contractile elements within the muscle.

1.2.6. Hyperresponsive airway smooth muscle contractility

The teleological role of smooth muscle in the airways remains contested, especially considering that no dysfunction or pathology is known to directly result from a loss of airway smooth muscle contractility [102]. To date, the most tempting explanation is that ASM maintains the tone of the airways [2]. Studies of isolated ASM strips have demonstrated a capacity for muscle shortening to by up to 90% of the optimal muscle length (l_o) [113]. By extrapolation, airway closure *in vivo* would occur before such an extent of muscle shortening *in vitro*, as described previously.

Studies on isolated muscle strips from hyperresponsive and normal airways have suggested that the intrinsic mechanical properties of the ASM is different, as no difference in ASM mass was found [52]. The key role that ASM plays in airway hyperresponsiveness is patent in that it is characterized by many of the same criteria that define airway hyperresponsiveness itself: the ASM of these airways are both hy-

persensitive and hyperreactive to contractile agonists [56,86], and have an impaired capacity for relaxation [56].

Compelling evidence is emerging that the velocity of shortening differs in asthmatic ASM, and is therefore more appropriate for assessing ASM hypercontractility than isometric force, given the conflicting results that have been published with the latter [107,114]. Furthermore, a number of studies have shown that both the rate and maximal extent of muscle shortening are enhanced in hyperresponsive ASM, as shown in models of sensitized [52,59,87] and innately hyperresponsiveness airways [8,36]. Work on human ASM has also shown a greater velocity of muscle shortening in sensitized [88] and asthmatic airways [11,81]. Indeed, a greater velocity of shortening of ASM contractility could very well be responsible for the rapid re-narrowing of asthmatic airways following a DI, resulting in a very brief bronchodilation [31].

Several hypotheses have been proposed to explain the well-characterized differences in contractile behavior of hyperresponsive ASM. The first is that the intrinsic properties of the contractile machinery of hyperresponsive ASM itself are different [41]. Second, it has been suggested that the intracellular signaling pathway regulating the activity of the contractile elements in ASM has been modified, either by an increased propensity for activation in response to a given stimulus, a greater response to recruit a larger population of contractile elements, or both [98].

1.3. SMOOTH MUSCLE

1.3.1. Introduction

Smooth muscle is a tissue of mesodermal origin, lining the hollow organs of the body, such as the digestive tract, blood vessels, and airways. Naturally, there are differences in the functioning of each organ, sometimes within the same organ, and these differences are reflected in the contractility of the respective smooth muscle lining that organ. Such variations in contractility determine functions, such as maintenance of vessel diameter or peristaltic movements in the gut. Workers in smooth muscle research have classified the various smooth muscles into two types: tonic and phasic. The different smooth muscle types had been classified previously according to their electrophysiological properties into single-unit and multi-unit, which will be described later. The current classification of phasic or tonic stratifies smooth muscle tissues according to their contractility and the nature of their contractile response. Considerable work has been devoted to investigate the mechanisms responsible for imparting the difference in contractility between these two muscle types, and these differences can provide insight into how the contractility of ASM in airway hyperresponsiveness becomes enhanced.

1.3.2. Smooth muscle types

1.3.2.1. Phasic smooth muscle

Phasic muscles are those that have traditionally been described to be present in the visceral organs, as in the lining of the stomach, small intestine, colon, as well as the bladder, portal vein, and other smaller blood vessels, such as metarterioles. This muscle type has been described as single-unit, with extensive cell-to-cell contacts by gap junctions and relatively little innervation [63,113]. This muscle type is characterized by significant myogenic activity by pacemaker cells that induces waves in the electric potential of the surrounding myocytes through the extensive gap junction network. The peak of these waves usually results in action potentials, distinguishing this muscle type from multi-unit muscles [109]. Peristaltic contraction of digestive tract muscles are a good example of the waves of contraction of this muscle type, and contractions are relatively short and fast compared to tonic muscles. Although work on the contractile parameters of phasic and tonic smooth muscles is lacking, it has been shown that phasic muscles have an up to 20-fold greater velocity of maximal shortening compared to tonic muscles [91].

1.3.2.2. Tonic smooth muscle

Tonic muscles were originally described as multi-unit, to illustrate the relatively extensive neural influences and close nerve-muscle contacts that regulated contractility, with relatively few gap junctions between the individual smooth muscle cells (SMC) [63,113]. Thus, contraction in this muscle type is not uniform, but rather contracts in multiple units and does not exhibit action potentials. The current classification as tonic relates to the slow, yet tone-maintaining nature of the contractile response [109]. This tone-maintenance is accomplished with minimal energy cost. Given the ability of this muscle to maintain force with minimal energy expenditure, this muscle type is commonly found lining the large vessels of the vasculature, such as the aorta and vena cava, gravid uterus, and in the sphincters such as the lower esophageal and gastric sphincters.

A study comparing the rates of relaxation of phasic and tonic muscles reported that tonic muscles possessed a slower time course of relaxation. In addition, the time course of muscle relaxation was found to be more significantly affected by varying concentrations of MgADP compared to that in phasic muscles [43]. The greater sensitivity of tonic muscles to MgADP concentrations implies that the molecular contractile machinery of tonic muscles possesses a greater affinity for ADP compared to that in phasic muscles. Indeed, a slower rate of ADP release was suggested for dephosphorylated cross-bridges in tonic muscles compared to phasic, and

this difference was thought to explain the greater force maintenance of this muscle type [66,67].

1.3.2.3. Airway smooth muscle

It has been postulated that ASM contraction is continually being prevented in healthy airways; hence, the designation of ASM by some workers as a “frustrated” organ [102]. To add to its intrigue, the classification of ASM as tonic or phasic is conflicting. Functionally, it has been classified with multi-unit smooth muscle tissues, although morphologically, ASM appears to resemble single-unit smooth muscles due to its relatively poor innervation and abundance of gap junctions [63]. N.L. Stephens has assigned ASM to a category intermediate between tonic and phasic [113].

1.3.3. Smooth muscle contractility

Considerable work has been devoted to identify the mechanisms underlying the difference in phasic and tonic contractions, and this has included investigations of protein expression and/or signaling pathways. The hope is that this will also provide insight into the specific mechanisms that mediate smooth muscle contractility.

1.3.3.1. Thick and thin filaments, cross bridge cycling

As is true for striated muscles, contractility is generated by the interaction of thick and thin filaments. The thick and thin filaments in muscle are composed of myosin and actin units, respectively. Their sliding activity is the result of cross bridge cycling, whereupon a conformational change in myosin is induced in an ATP-dependent process. Unlike striated muscles, smooth muscle thick and thin filaments do not arrange in well-defined sarcomeric structures, hence their “smooth” appearance. Rather, the actin filaments are attached to so-called dense bodies, located sporadically throughout the smooth muscle cell. It is likely that this loose arrangement of contractile filaments is related to their relatively labile nature, as mentioned earlier.

The onset of contraction in smooth muscle is quite distinct from striated muscle, in that it is principally initiated by phosphorylation of the myosin thick filaments, as opposed to calcium binding of actin filament proteins in striated muscles. Moreover, the regulation of contraction in smooth muscle is complex, as a number of different mechanisms have been described that regulate myosin phosphorylation, as well as some involvement of the actin-filament associated proteins [50].

1.3.3.2. Smooth muscle myosin

Myosin is functionally responsible for producing the contractile response in all muscles. Though smooth muscle myosin has a slower rate of ATPase activity than skeletal myosin, it actually exerts a greater average force than skeletal muscle myosin, as tested at the molecular level [124]. This is in agreement with a study showing that smooth muscle produces greater force per cross-sectional area than striated muscle, even though the former contains less than a fifth of the myosin content [90]. Moreover, smooth muscle contraction is far more efficient than that of striated; ATP consumption in contracted smooth muscle is quite modest compared to that of striated muscles [91].

Smooth muscle myosin is a hexameric mechanoenzyme composed of two heavy chain polypeptides associated with four light chains (Fig. 1). The heavy chain molecule can be anatomically divided into three parts, proceeding from the amino to the carboxyl terminus: a large globular head region possessing the ATPase and actin-binding activities, a neck region, and a tail region. During the cross bridge cycle, the actin-bound myosin head pivots about the neck region in the power stroke, thus shifting the position of the actin filament and forming the basis of muscle contraction. The tail region is involved in assembly of the myosin molecules into thick filaments.

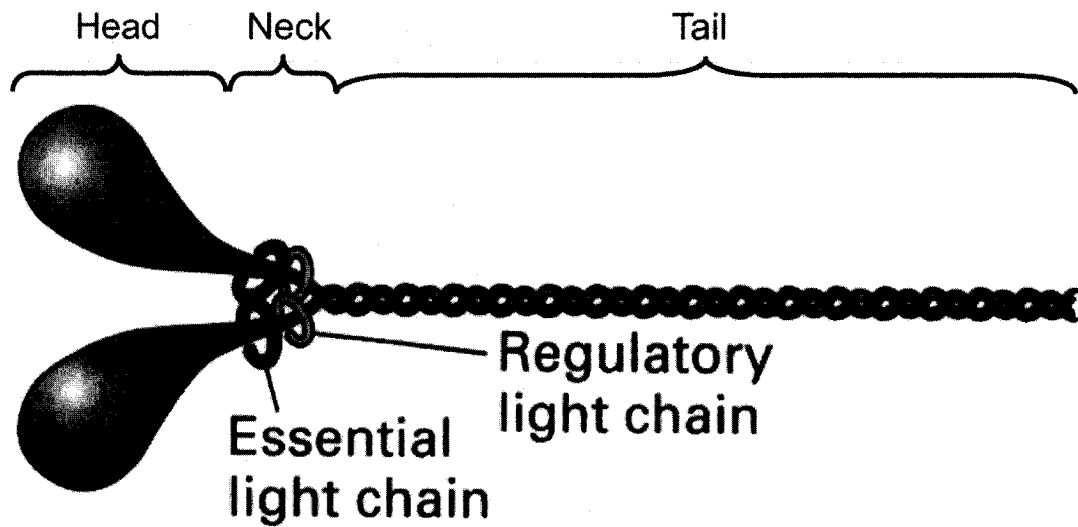


Figure 1: Smooth muscle myosin.

A schematic of the smooth muscle myosin heavy chain protein is shown, along with the two associated light chains. Phosphorylation of the regulatory light chain (LC_{20}) results in activation of myosin, enabling its ATPase activity and priming it for cross bridge cycling. Figure adapted from [1].

1.3.3.2.1. Myosin activation

The process of smooth muscle activation has been reviewed [50]. The predominant path of smooth muscle activation is by increased intracellular Ca^{2+} levels, similar to that in striated muscles. This process is chiefly orchestrated by way of a receptor-dependent IP_3 -signaling pathway, culminating in the release of intracellular Ca^{2+} stores from the sarcoplasmic reticulum. Extracellular Ca^{2+} channels can also contribute to the rise in intracellular Ca^{2+} levels. Unique to smooth muscle, the free Ca^{2+} ions bind to the ubiquitous signaling protein calmodulin, which in turn activates the enzyme myosin light chain kinase (MLCK). Activated MLCK in turn activates myosin by phosphorylating the 20 kDa associated light chains (LC_{20}) at the cost of 1 ATP. Phosphorylation of these light chains acts as the ON/OFF switch of smooth muscle myosin activity, hence their common description as the regulatory light chain (Fig. 1). Ca^{2+} influx results in LC_{20} phosphorylation, activating myosin and effecting contraction of smooth muscle.

To determine whether there are any differences in the intrinsic nature of the contractile machinery between phasic and tonic smooth muscles that was not due to differences in LC_{20} phosphorylation, Horiuti et al. maximally activated the LC_{20} 's by thiophosphorylation. This experiment involves phosphorylating the LC_{20} 's with the ATP analog $\text{ATP}\gamma\text{S}$, where the thiophosphate is less prone to dephosphorylation by myosin light chain phosphatase. The authors noted that even under conditions of

maximal myosin LC₂₀ activation, phasic smooth muscle mounted a greater rate of force development compared to tonic muscle [49]. Previous work involving striated muscles determined that the differences in shortening velocity between muscles were due to differences in content of the skeletal myosin isoforms in these muscles [125]. Therefore, variations in smooth muscle contractility could plausibly be due to a difference in content of the smooth muscle myosins.

1.3.3.2.2. C-terminal SMMHC isoforms

The smooth muscle myosin heavy chain (SMMHC) is expressed from a single gene (MYH11). Four different SMMHC isoforms have been characterized as arising from alternative mRNA splicing at two sites of the MYH11 transcript. One site of alternative splicing occurring in the tail region (Fig. 1) at the carboxyl terminus generates two products that differ by a sequence of 43 or 9 unique amino acids. These SMMHC isoforms are designated SM1 and SM2, respectively. A comparison of SM1 and SM2 rate of actin filament movement in the *in vitro* motility assay found no difference between isoforms [64]. Instead, they are thought to differ in their assembly into thick filaments, with the shorter SM2 isoform forming less stable filaments of myosin [99]. However, it remains to be seen whether this postulated difference in thick filament assembly between the SM1 and SM2 isoforms could affect

actin motility, since all *in vitro* motility studies have been performed with monomers of SM1 and SM2.

1.3.3.2.3. N-terminal SMMHC isoforms

Alternative splicing of a 21 base pair (bp) exon in the head region (Fig. 1) located near the 25/50 kDa junction generates two isoforms that differ by the presence or absence of a 7 amino acid sequence, designated (+)insert or (-)insert, respectively [46,130]. These isoforms can combine with either of the tail isoforms, generating four possible isoforms of SMMHC. Like those sequences that encode the SM1 and SM2 variants, the sequence of this 7 amino acid insert is highly conserved among the various species thus far studied [7], underscoring the significance of these isoforms to normal smooth muscle function.

The N-terminal isoforms have received considerable attention in the literature as the specific expression of these isoforms was correlated to smooth muscle type; the inserted isoform was described to predominate in phasic muscles, compared to more non-inserted isoform in tonic muscles [130]. Shortly after the isoforms were described, it was demonstrated that myosins from phasic muscles (predominating in (+)insert isoform expression) possessed a higher ATPase activity and propelled actin filaments with a greater velocity compared to tonic muscles (more (-)insert isoform) in the *in vitro* motility assay [65].

Using a laser trap, Lauzon and coworkers [72] were the first to provide more detailed insight into the functional effects of the insert sequence and showed that the faster rate of actin filament movement of the (+)insert isoform was due to a reduced time of myosin attachment to actin. However, unitary force production and unitary displacement were similar for the two isoforms, and the authors concluded that the insert affects the kinetics rather than the mechanics of the myosin molecule [71,72]. While the exact 3-dimensional structure of the insert sequence remains to be determined, a mutational study using chimeric myosins found that the length and flexibility of the insert loop were correlated with the rate of ADP release, the rate-limiting step in cross bridge cycling [115]. Given the expression pattern of the SMMHC isoforms and given that tonic and phasic muscles appear to differ in their affinity for ADP, it seems plausible that, as in striated muscles, the myosin isoforms play a prominent role in determining the mechanics of smooth muscles.

1.3.3.2.4. SMMHC isoform tissue expression

The expression of the SMMHC isoforms in the various smooth muscles has been reviewed [79,108]. However, the content of the SMMHC isoforms is not fixed in muscle tissues. Rather, the expression of all four SMMHC isoforms is regulated, and has been shown to change depending on smooth muscle development status [80,131,132], hormone level [16,77,89,110], and pathology [18,60,76,84,104,129]. In-

deed, correlation of the proportion of SMMHC (+)insert isoform expression to smooth muscle contractility has been demonstrated at the level of single myocytes [34] and whole muscle tissue [17].

The most convincing evidence thus far for the significance of the amino-terminal isoforms to smooth muscle contractility has come from a mouse knockout of the insert sequence from the SMMHC [6]. With one exception [96], differences in contractility of smooth muscle from various organs have been reported in this knockout animal. While the expression of most contractile proteins was shown to be unaffected in this model, the rate of force development of bladder muscle and velocity of shortening of mesenteric vessels were both decreased in the knockout animal [6]. A subsequent study showed reduced rate of bladder muscle shortening in the knockout [6]. Interestingly, the total isometric force of bladder muscle strips was also found to be reduced in the knockout animal [6], which seems difficult to explain since there is no difference in unitary force production between the isoforms [72]. However, the authors pointed out that these studies were performed on *in vitro* motility assays using monomeric myosins, and that *in vivo*, the mechanics of filaments of a particular isoform of myosin may allow for such differences in isometric force [6].

Tuck et al. examined the pulmonary mechanics of this knockout animal, and the time course of bronchoconstriction was found to be longer for the knockout compared to the wild type mouse. While the differences in time course of bronchoconstriction were modest, no changes to airway mechanics were reported [122].

Tuck and coworkers pointed out that the parent strain had previously been categorized as being hyporesponsive in a strain survey of airway reactivity [30]. It may therefore have been very difficult to discern a decrease in airway responsiveness in an already relatively hyporesponsive animal.

1.3.3.2.5. Smooth muscle myosin 17 kDa light chain isoforms

The 17 kDa myosin light chain (LC₁₇) is associated with the neck region of the myosin heavy chain, adjacent to the regulatory light chains. The specific role that this subunit of myosin plays in contractility remains unknown, though it has been shown to be necessary to generate maximal force and velocity of actin filament propulsion in an *in vitro* motility assay, hence its designation as the “essential” light chain [123]. Two LC₁₇ isoforms generated by alternative mRNA splicing have been identified, differing by 5 unique amino acids at the C-terminus. These isoforms can be separated by isoelectric focusing, so the more acidic one is designated LC_{17a}, and LC_{17b} for the more basic one. While no functional difference has been observed when the isoforms were switched on myosins in the *in vitro* motility assay [100], others have indicated that a particular LC₁₇ isoform content follows muscle contractility in a manner similar to the N-terminal SMMHC isoforms. This expression pattern suggests a greater content of the LC_{17a} isoform in faster, phasic muscles, and a predominance of LC_{17b} in the slower, tonic muscles [47,83].

1.3.3.3. Actin filament-associated proteins

As mentioned earlier, the contractile response of smooth muscle is the result of interaction between myosin and actin filaments. The most commonly cited proteins that associate with the actin filament in smooth muscle are tropomyosin, *h*-caldesmon, and calponin. However, since smooth muscle is activated by phosphorylation of the myosin-associated LC₂₀'s, the involvement of these actin-decorating proteins on contraction is thus far thought to modulate contraction rather than initiate it.

Tissue-specific expression of these proteins has been suggested for phasic and tonic muscle tissues. It was shown that phasic muscles expressed a predominance of the *h*-isoform of caldesmon, whereas a greater content of the *l*- isoform was found in tonic muscle tissue [116].

1.4. FISHER & LEWIS RAT MODEL OF AIRWAY HYPERRESPONSIVENESS

The Fisher and Lewis rat model was established as a model of innate airway hyperresponsiveness based on greater intrinsic airway response evoked in the Fisher rats to bronchoconstrictive challenge compared to Lewis [26,35]. A number of studies have since addressed what differences exist in the airways of these animals that could be responsible for conferring the difference in airway responsiveness and a number of factors have been identified.

A greater airway smooth muscle content was found in the airways of Fisher rats, though this was suggested to contribute only partially to the difference in airway response, given that intra-strain variability in airway smooth muscle content was not correlated to intra-strain differences in airway responsiveness [35]. Explants of Fisher intrapulmonary airways were shown to be hypersensitive to contractile agonists, more commonly attained complete airway closure, and narrowed at a faster rate compared to Lewis airways [126]. No pre-existing conditions of inflammation or pathology have been noted in either rat strain [85].

The notion that the intrinsic contractility of Fisher and Lewis airway smooth muscle differs was substantiated by a finding showing that *in vitro* Fisher tracheal strips not only possess a greater sensitivity to contractile agonists, but also a greater maximal isometric force response compared to Lewis airways [56]. Recently, Blanc

and colleagues [8] showed that Fisher rat tracheal smooth muscle strips had a greater maximal velocity of unloaded shortening *in vitro* compared to Lewis tracheal smooth muscle. As maximal shortening velocity is determined by myosin ATPase activity [59], the authors used a modification of AF Huxley's model of cross bridges adapted to nonsarcomeric muscles and found that the kinetics of cross bridges differed between Fisher and Lewis tracheal smooth muscle. Specifically, they noted that Fisher cross bridges had a shorter duration of cross bridge attachment and detachment [8]. This could well be due to the difference in actin-attachment times already described for the SMMHC isoforms [72]. The finding by Blanc et al. [8] that the cross bridges in Fisher and Lewis rat tracheal smooth muscle differ in kinetics provides an interesting explanation for the discrepancy in muscle mechanics that has been well characterized at the muscle level. These differences could play a significant role in underlying the enhanced airway narrowing associated with airway hyperresponsiveness. In this thesis, I sought to determine whether a difference in the expression of SMMHC isoforms could explain the differences in contractility that have been reported in Fisher and Lewis rat ASM.

Other studies on the Fisher and Lewis rat model of airway hyperresponsiveness have proposed an alternative mechanism by which contractility becomes enhanced in the Fisher rats. This alternative suggests that an enhanced signaling response mechanism that results in a greater recruitment of myosins for contraction occurs in Fisher tracheal smooth muscle, and leads to its hyperresponsiveness. A

greater Ca^{2+} mobilization was found in Fisher TSM in response to contractile agonist [118]. This information thus suggests that the signaling response in Fisher ASM is capable of mounting a more substantial contractile response compared to the Lewis animal.

In this thesis, I sought to verify whether this increased Ca^{2+} mobilization was translating into greater LC_{20} phosphorylation, which is the final step of the smooth muscle activation response. The LC_{20} phosphorylation response to a stimulus was measured, which provides an index of the number of myosins recruited for contractions. A submaximal stimulus was chosen that would not lead to full LC_{20} phosphorylation, thus serving as an assessment of the reactivity of the muscle for that stimulus.

THESIS RATIONALE AND OBJECTIVES

THESIS RATIONALE: Hypercontractility of airway smooth muscle has long been suspected of playing a role in airway hyperresponsiveness, though conflicting reports regarding the contractility of asthmatic airway smooth muscle has cast some doubt on this [27,101,120]. However, the velocity of shortening, in turn determining the extent of smooth muscle shortening, is becoming increasingly recognized as the parameter to study such differences in contractility [3,8,11,81]. However, it remains unclear whether alterations in ASM contractility are the consequence of changes brought about by other circumstances, such as inflammation, or whether they serve more to predispose an individual to the development of airway hyperresponsiveness and asthma. Given the concordance between smooth muscle velocity of shortening and expression of the (+)insert and (-)insert SMMHC isoforms [17,34,73], I sought to assess the relevance of the SMMHC isoforms to a model of innate airway hyperresponsiveness. Also taken into account are the extent of myosin activation for contraction and the expression of other contractile proteins. The goal of this project, therefore, is to assess, at the molecular level, the factors that contribute to differences in ASM contractility in a model of innate airway hyperresponsiveness: the Fisher and Lewis rats.

THESIS OBJECTIVES FOR STUDY ON FISHER AND LEWIS RAT TRACHEAE:

1. Determine the relative expression of the SMMHC isoforms in the tracheae of Fisher and Lewis rats at the mRNA and protein levels.
2. Investigate the expression levels of other contractile proteins: actin, *h*-caldesmon, and the LC_{17a} and LC_{17b} isoforms.
3. Compare the extent of myosin activation in response to a sub-maximal cholinergic stimulus by measuring LC₂₀ phosphorylation levels.
4. Determine the functional role of the SMMHC isoform overexpression in airway SM hypercontractility, by measuring the velocity of shortening after eliminating differences in SM activation.
5. Sequence the (+)insert isoforms in humans.

CHAPTER II. MATERIALS AND METHODS

2.1. MATERIALS

2.1.1. Animals

Fisher (F344) and Lewis rats 8-12 weeks of age were purchased from Harlan (IN, USA) and housed in an animal care facility at McGill University before experimentation. All experimental protocols involving animals were approved by the McGill University Animal Care Committee and complied with the guidelines of the Canadian Council on Animal Care. Animals were sacrificed with an overdose of sodium pentobarbital (100 mg/kg, i.p.).

2.1.2. Reagents

Unless otherwise specified, all reagents and chemicals were obtained from Sigma-Aldrich, ON, Canada.

2.2. REAL-TIME QPCR OF (+)INSERT SMMHC ISOFORMS

Real-time quantitative PCR was carried out for the relative quantification of (+)insert SMMHC isoform and total SMMHC isoform expression. Ubiquitin C was used as a reference gene. Aortas, bladders, and tracheae were harvested from 8 Fisher and 8 Lewis rats, added to RNAlater buffer (Qiagen, ON, Canada) and homogenized. mRNA was extracted from the homogenized samples using the RNeasy Protect Mini Kit (Qiagen), and DNase was added to eliminate DNA contamination. mRNA was quantified by spectrophotometry absorbance at 260 nm wavelength. 0.5 μ g of RNA was reverse transcribed (Reverse Transcriptase Kit, Qiagen). PCR reactions were performed in a volume of 20 μ l containing 1 μ l of cDNA, 10 μ l of 2x QuantiTect SYBR Green PCR (Qiagen), 7 μ l of nuclease-free H₂O, and 1 μ l of both the forward and reverse primers (final concentration 0.1 μ mol each). The samples were amplified in a LightCycler system (Roche Diagnostics, QC, Canada). The real-time PCR conditions consisted of a denaturation step of 15 min at 95 °C, followed by an amplification of 45 cycles (denaturation at 95 °C for 15 s, annealing at 60 °C for 20 s, and extension at 72 °C for 20 s) and 1 melting curve cycle. The following primer sets were used: (+)insert SMMHC isoform-specific forward primer 5'-CAAGGCCCATCTTTTGCCTAC-3'; total SMMHC forward primer, 5'-CCAATCCTGGAGGCTTTCG-3'; common reverse primer for (+)insert and total SMMHC, 5'-CTCTCGTCCCTAGCATGTC-3'; forward ubiquitin C (UBC) primer,

5'-GGCATGCAGATCTTTGTGAA-3'; reverse UBC primer, 5'-AGGGTGGACTCCTTCTGGAT-3'. All primers were obtained from Invitrogen. Each primer set generated only one PCR product.

Aorta and bladder smooth muscles were taken as representative tonic and phasic smooth muscle tissues, respectively, to validate the specificity of the (+)insert and total SMMHC primer sets. A (-)insert-specific primer set could not be made, however, due to a poor G-C base pair content in the regions flanking the insert site. Nevertheless, expression of (+)insert isoform was corrected to total SMMHC to provide an index of the proportion of the (+)insert isoform in the various smooth muscle tissues.

2.3. WESTERN BLOT OF CONTRACTILE PROTEIN EXPRESSION

2.3.1. Tissue preparation

Whole tracheae from five Fisher and five Lewis animals were harvested, and dissected free of loose connective tissue and blood vessels in ice-cold saline. Tissues were then flash frozen in liquid nitrogen, and homogenized using a mortar and pestle. The homogenates were then put in extraction buffer containing sodium pyrophosphate, glycerol, EDTA (Fisher Scientific, ON, Canada), EGTA (Fisher Scientific), β -mercaptoethanol, and a cocktail of protease inhibitors at a pH of 8.8. Samples were left on ice for 1 hr to complete the extraction process, and then centrifuged at 14,000 RPM for 30 min. The pellet was discarded, and the protein concentration of the supernatant was determined using Bradford Reagent. Bromophenyl blue stain and a final concentration of 10% glycerol were added to the extract before loading for gel electrophoresis, and equivalent amounts of protein were loaded per gel. Mini-gels of polyacrylamide were prepared: 4% acrylamide for the stacking gel and 7% for the running gels. The gel electrophoresis was run at 100 V for 2 hrs, and proteins were then transferred overnight onto polyvinylidene fluoride (PVDF) membranes (Bio-Rad, ON, Canada) at 60 V. Since all samples from each strain were run on the same gel, the gel and Western blotting was run in triplicate to con-

trol for variations within the experimental procedure. When not in use, protein extracts were kept at -80 °C.

2.3.2. Western blot of (+)insert and total SMMHC

PVDF membranes were first blocked with 1% bovine serum albumin for 1 hr. (+)insert SMMHC isoform expression was probed using an antibody specific to the 7 amino acid insert sequence. To improve the sensitivity and resolution of the immunoblot signals for the (+)insert-specific SMMHC, a biotinylated secondary antibody (DakoCytomation, ON, Canada) was used. The secondary antibody was detected by a streptavidin-biotinylated horseradish peroxidase (HRP) complex (GE Healthcare Biosciences, QC, Canada) and Enhanced Chemiluminescence (ECL) reagent (GE Healthcare Biosciences). These membranes were subsequently stripped in a solution containing 62.5 mM Tris-HCl, 10% SDS, and 0.7% β -mercaptoethanol, and incubated in a water bath shaker for 30 min at 60 °C. At the end of the 30 min, the membranes were rinsed vigorously with Tris-buffered saline with Tween (TBS-T), and then probed with an antibody recognizing all isoforms of SMMHC.

2.3.3. Western blot of actin, caldesmon, and LC₁₇ isoforms

Expression of actin, *h*-caldesmon, and GAPDH were also probed on the same membranes, with the latter used as a reference protein. Both total SMMHC and *h*-caldesmon expression were detected using biotinylated secondary antibodies for more robust signal detection. Actin and *h*-caldesmon expression were detected using an anti-mouse antibody conjugated with HRP (GE Healthcare Biosciences). Again, these bands were visualized with ECL, and relative quantification of all the Western blots was performed by densitometry analysis (Fluorochem 800, Alpha Innotech, CA, USA).

Expression of the 17 kDa essential light chain (LC₁₇) isoforms was determined on three rats of each strain. Tracheae were harvested, as above, and placed in non-denaturing conditions [106] (*personal communication Sobieszek, A*) after homogenization in liquid nitrogen. Briefly, proteins were extracted in a non-denaturing extraction buffer composed of 8.5 M urea and 0.5% β -mercaptoethanol, and run on 10% acrylamide urea-glycerol gels. The LC_{17a} and LC_{17b} isoforms were separated, transferred onto nitrocellulose membranes (Bio-Rad), and later identified using an antibody recognizing both LC₁₇ isoforms and quantified as described above. Alternatively, the expression of the LC₁₇ isoforms was also determined by directly staining non-transferred gels with GelCode Blue reagent (Biolynx, ON, Canada).

2.3.4. List of antibodies

The following polyclonal antibodies were used for quantifying the (+)insert and total SMMHC expression: (+)insert SMMHC Ab (kind gift of Dr. A. Rovner, University of Vermont, VT, USA) and total SMMHC BT-562 Ab (Biomedical Technologies, MA, USA). The remaining monoclonal antibodies were as follows: actin Ab (clone AC-40, Sigma, ON, Canada), caldesmon Ab (clone C-21, Sigma), GAPDH Ab (Ambion, TX, USA), and LC₁₇ Ab (kind gift of Dr. M. Periasamy, Ohio State University, OH, USA).

2.4. SEQUENCING OF THE HUMAN (+)INSERT SMMHC ISOFORM

2.4.1. Identification of the human (+)insert

Given that SMMHC is a highly conserved protein, a sequence corresponding to where the 21 bp insert locates in other species' SMMHC was found in the human (-)insert SMMHC (GenBank accession no. NM-002474). 1 μ g of human bladder total RNA (BD Clontech, CA, USA), in a total reaction volume of 20 μ l, was reverse transcribed with oligo(dT)₁₂₋₁₈ primer, Superscript II, and RNAGuard ribonuclease inhibitor (GE Healthcare Biosciences). The following primers flanking this hypothetical region containing the code for the insert were designed: sense primer 5'-CCGAAAACACCAAGAAGGTC-3', antisense primer 5'-GTTGGCTCCCACGATGTAAC-3'. cDNA from a tissue bank of human bladder smooth muscle was amplified with the primers, and two products resulted that differ by only a small number of nucleotides. Sequencing of the products showed one to be the transcript corresponding to the non-inserted isoform, while the other was shown to include an additional 21 nucleotides of the exact sequence as shown in rats [7].

2.4.2. Sequencing of the full-length (+)insert isoforms

The full-length transcript of the myosin isoforms containing the 5' insert was amplified in four segments (1.8 kb each) by conventional PCR, and the products were sequenced. The entire (+)insert SMMHC transcript was amplified, and the product was then used in nested and hemi-nested PCR to yield four overlapping segments. All primers were designed from human (-)insert SM1 SMMHC (GenBank accession no. NM-002474). The PCR mixture consisted of 2 mM MgSO₄, 1x High Fidelity PCR buffer (Invitrogen), each dNTP at 0.2 mM, 1 unit of High-Fidelity Platinum *Taq* (Invitrogen), each of the forward and reverse primers for the SMMHC gene at 0.2 μ M, and 1 μ l of the above-described cDNA strand. Amplification was performed for 35 cycles (1 min of denaturation at 94 °C, 1 min of annealing at 55 °C, 80 s of extension at 68 °C per kilobase of amplification target) and 40-min final extension at 68 °C. The PCR amplification products were resolved on 0.8% TAE-agarose gel electrophoresis and visualized by ethidium bromide. Fragments were cloned and commercially sequenced.

2.5. LC₂₀ PHOSPHORYLATION TO SUB-MAXIMAL STIMULUS IN FISHER AND LEWIS RAT TRACHEAL SMOOTH MUSCLE

2.5.1. Trachealis Contractility:

Measurement of ASM contractility were taken from the tracheae, as this organ has been previously been described to be representative of the peripheral airways in the Fisher and Lewis rats [56]. Tracheae were dissected from the carina to the bronchial bifurcation. They were immediately placed in ice-cold Krebs-Henseleit solution (K-H), prepared as in [40] with the modification of 10 mM glucose. Tracheae were then dissected free of blood vessels and any loose connective tissue. To best measure the isometric force of each trachea, tracheae were sectioned into four equivalent segments of about 4 mm in width. A longitudinal cut was made through the ventral side of the trachea through the cartilage rings, and 4-0 silk suture thread passed through the cartilaginous portion of one of the tracheal segments. A loop was made of the thread and hooked onto a Grass FT03 C force transducer (Grass-Telefactor, MA, USA). The other cartilaginous end was affixed to an alligator clip, and positioned in a 25 ml Radnoti organ bath filled with K-H bubbled with 95% O₂, 5% CO₂ at 37 °C. Four bath systems and transducer setups were used, such that all tracheal segments were studied simultaneously. Fresh K-H was instilled ap-

proximately every 10 min, and incubated for 30 min. Data acquisition was performed using LABDAT software (RHT-InfoDat, QC, Canada).

A dose-response to MCh was performed on three animals of each strain, and a concentration of 10^{-6} M was chosen for producing a submaximal response in both strains of rats (thereby avoiding saturation of the force and phosphorylation signals). Two to three segments per rat were stimulated, while the most cranial segment was kept as a control: mounted in the tissue bath but not challenged with MCh. The muscle was allowed to contract for 30 s in response to this dose, freeze-clamped with forceps cooled in liquid N₂, and placed for 2 min in a mixture of 10 mM dithiothreitol (DTT) and 10% trichloroacetic acid in acetone to arrest intracellular enzymatic processes, so as to preserve the state of LC₂₀ phosphorylation. It was then transferred to an extraction buffer for Western blotting.

2.5.2. LC₂₀ Phosphorylation Analysis

Tracheal segments were pulverized in liquid nitrogen and homogenized at 4 °C in a 10% sodium dodecyl sulfate (SDS) extraction buffer with 5% β-mercaptoethanol and a cocktail of protease inhibitors. Protein concentration was determined using the Bradford assay (Bio-Rad, ON, Canada) on a 96-well plate. Western blot analysis of LC₂₀ content and phosphorylation was performed on pairs of Fisher and Lewis rats. The extracts were resolved on 15% polyacrylamide gels

run for 2 hours at 100 V, and transferred to nitrocellulose membranes (Bio-Rad). The two antibodies used were: LC₂₀ (Santa Cruz Biotech, CA, USA) and phosphorylated LC₂₀ (pLC₂₀) (Cell Signaling Tech., MA, USA). Baseline phosphorylation was determined in the non-stimulated strips. Thiophosphorylated chicken gizzard extract was used as a positive control. The results are expressed in relative units normalized to the darkest band on each blot. The average values of LC₂₀ expression and phosphorylation for all stimulated strips from each animal were used in the final comparison of LC₂₀ expression and phosphorylation between rat strains.

2.6. MUSCLE STRIP MECHANICS AND THIOPHOSPHORYLATION

2.6.1. Muscle strip preparation

To dissect out the relative contribution of myosin isoforms vs. light chain activation to the hyperresponsiveness of the Fisher compared to the Lewis rats, I set up a quick-release apparatus with a dual-mode force transducer and high-speed length controller system (Model 300B-LR, Aurora Scientific Inc., ON, Canada) with a horizontal multi-bath setup. This allows for the rapid changing of solutions of the muscle strip. Rat tracheae were dissected from the larynx to the carina as described previously and immediately transferred to ice-cold K-H solution, pH 7.4, aerated with 95% O₂, 5% CO₂. A segment spanning 3 cartilage rings was excised near the carina and opened by a longitudinal cut through the cartilage rings opposite to the tracheal muscle, such that the muscle strip bridging the two cartilaginous segments measured about 2-3 mm wide, 2 mm long, and 0.2 mm thick. The epithelial lining was removed by gentle rubbing with a cotton swab, and the tracheal strip mounted by passing, directly through the cartilage rings, stainless steel hooks that were on one side attached to the lever arm and on the other side, to a fixed point. (Hooks were passed as close to the muscle as possible to minimize the contribution of connective tissue compliance). The muscle was perfused with 95% O₂ / 5% CO₂-saturated K-H

at 37 °C at a flow rate of ~2 mL/min. For intact muscle strip measurements, a horizontal bath system with a water jacket was used to maintain the bathing solution at 37 °C. For permeabilized experiments, another bath system was used and experiments were conducted at room temperature.

2.6.2. Intact muscle strip measurements

Prior to the thiophosphorylation experiments, parameters of contractility such as isometric force and maximal velocity of shortening were first measured to compare with previously reported data [8]. All experiments were made and analyzed using the Dynamic Muscle Control and Analysis software (Aurora Scientific Inc.), and a Grass S48 AC stimulator (Grass-Tele-Factor) was used for electric field stimulation (EFS). An EFS (20-30 V) of 10 s duration was used, which was just long enough for the muscle to generate a stable isometric tension. Muscle strips were equilibrated by EFS every 4 min over a period of about 90 min, during which muscle length was increased in 0.25 mm increments 1 min prior to EFS. As such, a length-tension relation was built for each muscle strip. A 4-parameter Weibull function was fit to each curve and the optimal muscle length (l_o) and maximal isometric tension (P_o) were derived [127].

To obtain the maximal velocity of shortening for each muscle strip, force-velocity curves were made by performing a series of quick-releases on the muscle

[62]. Briefly, the muscle was clamped to various loads between 3% and 75% of P_o 0.7 s after the onset of EFS, and the muscle was allowed to shorten for about 1 s until the stimulation was terminated. The clamp to the afterload was accomplished within 50 ms. The rate of shortening was then derived from the ensuing change in length, and a complete F-V relation was created by repeating these measurements at various afterloads. To extrapolate the maximal rate of shortening (V_{max}), where there is theoretically zero load on the muscle, the data was fit to Hill's equation [48]:

$$V = b (P_o - P) / (a + P)$$

where V corresponds to the velocity of muscle shortening, P is the force produced by the muscle, and a and b are constants. Due to a brief oscillation of the lever arm in clamping to the specified afterload during quick release, the rate of shortening measurements are taken 100 ms after the release, when oscillations have subsided. The rate of shortening is obtained by deriving the slope of a 50 ms interval 100 ms after the release.

2.6.3. Muscle permeabilization and thiophosphorylation

Relaxing solutions, Ca^{2+} -stimulating solutions, and rigor solutions were prepared using recipes adapted from those published previously [67]. All solutions were

buffered to pH 7.1 with 30 mM piperazine-1,4-bis(2-ethanesulfonic acid) (PIPES), 1 mM DTT, kept at 0.2 M ionic strength with potassium methanesulfonate, at room temperature, and the concentrations used are indicated in Table 1. First, the muscle was transferred to a bath containing G2 solution and 75 μ M of β -escin at room temperature for 30 min. The saponin ester β -escin is a suitably mild permeabilizing agent that allows nucleotides and some intermediate-sized proteins to transit through the extracellular membrane while maintaining the receptor to intracellular signaling coupling intact [51]. The muscle was then washed several times with the relaxing solution G10. Contractility of the permeabilized muscle fiber was verified by transferring the muscle to the pCa 4.5 solution CaG containing, 5 μ M calmodulin (CaM).

For muscle thiophosphorylation, intracellular Ca^{2+} stores were first depleted by incubating fibers in 10 μ M of the calcium ionophore A23187 for 10 min. ATP was then depleted from muscle fibers by repeated washing with the Rigor solution. The fibers were then thiophosphorylated with 2.1 mM $\text{ATP}\gamma\text{S}$, in a solution of Ca^{2+} and 5 μ M CaM for 10 min. The thiophosphorylated muscle was then washed free of $\text{ATP}\gamma\text{S}$ by repeated washing with Rigor solution. The muscle was then allowed to contract by transferring to G10 solution, and the time to half-maximal force development ($t_{1/2}$) measurements were made on the ensuing contractile response, as shown previously [49].

Solution	pCa	Na ₂ CP	Na ₂ ATP	MgMs ₂	KMs	K ₂ EGTA	CaEGTA	CPK
G2	9	10	5.2	7.3	74.1	2	0	0.1 mg/mL
G10	9	10	5.1	7.9	46.7	10	0	0.1 mg/mL
CaG	4.5	10	5.2	7.3	47.1	0	10	0.1 mg/mL
Rigor	0	0	0	0	90	1	0	0
Ca- Rigor	4.5	0	0	0	90	0	10	0

Table 1: Table of reagents used for permeabilized muscle strips (in mM).

The following recipes of solutions serve to mimic intracellular conditions and allow for the tight control of intracellular Na₂ATP and free Ca²⁺ levels, and are adapted from a previous study [67]. 1 mM DTT and 30 mM PIPES were added to all solutions. Ms, methanesulfonate; CP, creatine phosphate; CPK, creatine phosphokinase.

2.7. STATISTICS

For a more stringent analysis of the data, non-parametric Mann-Whitney tests were performed on the (+)insert, total SMMHC, actin, *h*-caldesmon, and LC₁₇ isoform protein expression, since a small number of animals were used from each strain. Paired t-tests were performed for analysis of LC₂₀ expression and phosphorylation. All remaining data sets were analyzed using unpaired t-tests. A value of $p < 0.05$ for each test was interpreted as significant. All data are reported as mean \pm dSE.

CHAPTER III. RESULTS

3.1. REAL-TIME QPCR EXPRESSION OF (+)INSERT SMMHC ISOFORMS IN FISHER AND LEWIS RATS

The mRNA expression of the (+)insert isoform and total SMMHC were analyzed from the aorta, bladder, and trachea from 8 sets of Fisher and Lewis animals (Fig. 2). The ratio of (+)insert content to total SMMHC in the aorta of both strains was relatively low, and no significant difference was found between the Fisher and Lewis rats ($0.023 \pm d0.014$ vs. $0.005 \pm d0.001$, respectively). The highest ratio of (+)insert content, relative to total SMMHC, was seen in the bladder muscle. Again, no significant difference was found between the strains ($0.33 \pm d0.06$ vs. $0.39 \pm d0.08$, respectively). This expression pattern is consistent with what has been previously reported for (+)insert SMMHC isoform expression in tonic versus phasic muscle tissues, validating the specificity of the primers. In the trachea, the content of the (+)insert isoform was intermediate between the aorta and bladder. However, a strain difference was found when the ratio of (+)insert to total SMMHC was compared between the two strains. A significantly greater (+)insert content was found in the hyperresponsive Fisher trachealis ($0.24 \pm d0.03$) compared to in the Lewis ($0.12 \pm d0.01$) ($p < 0.01$). Expression of the housekeeping gene, ubiquitin C, was similar for all tissues and between the strains (data not shown).

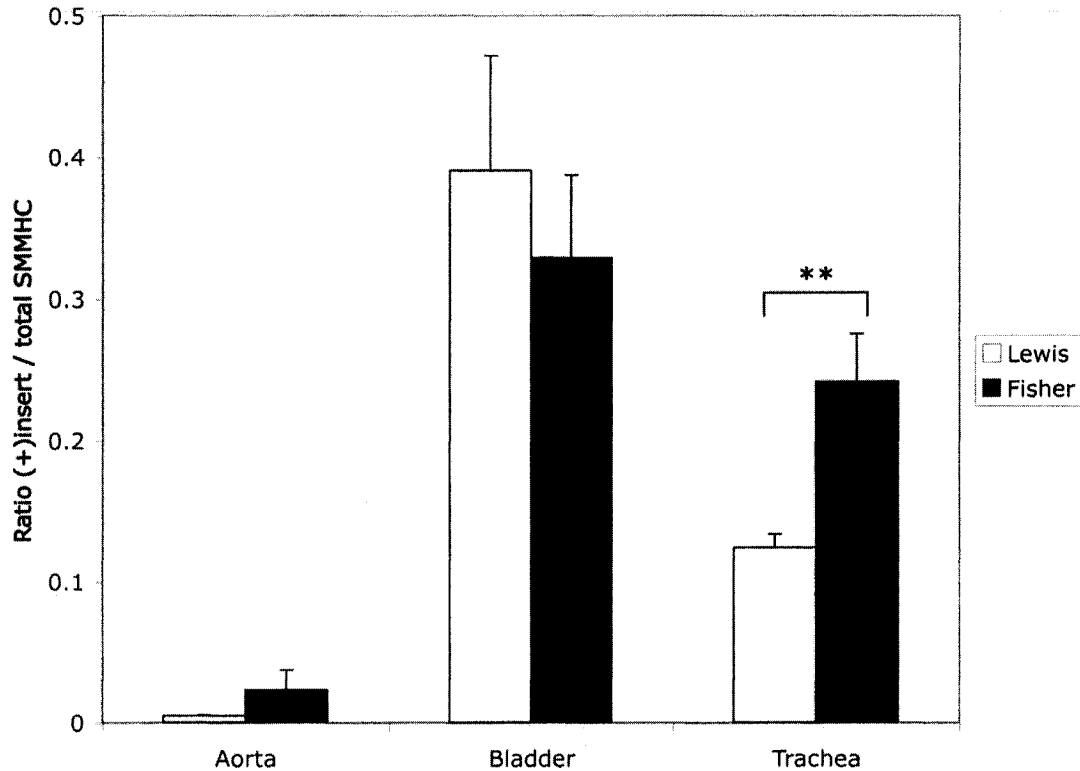


Figure 2: Expression of (+)insert isoform mRNA content in Fisher and Lewis rat smooth muscle.

mRNA expression of (+)insert isoform and total SMMHC was quantified by real-time QPCR in smooth muscle from the Fisher and Lewis rats. The ratio of (+)insert isoform expression to total SMMHC expression is shown. Aortas were used as a control for low (+)insert content, whereas the bladder, being a phasic muscle, was a control for high content of the (+)insert isoform. n=8 for each strain.

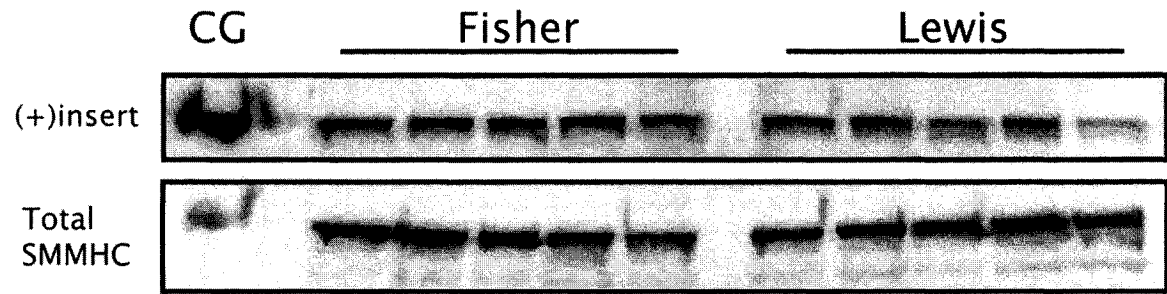
****p<0.01**

3.2. CONTRACTILE PROTEIN EXPRESSION

The content of the (+)insert isoform in the tracheae of Fisher and Lewis rats was assessed by normalizing the expression of the (+)insert isoform to the total SMMHC content of the subsequently stripped membrane. The value of (+)insert isoform expression normalized to total SMMHC was found to be significantly greater in the tracheae of the relatively hyperresponsive Fisher animal compared to the Lewis strain (1.84 ± 0.10 vs. 1.27 ± 0.06 , respectively, $p < 0.01$) (Fig. 3). However, expression of total SMMHC was not found to differ between the rat strains, when normalized to GAPDH (1.14 ± 0.11 vs. 1.00 ± 0.02 , respectively).

Similarly, the expression of other contractile proteins did not differ in the tracheae of Fisher and Lewis rats. No difference was found in the content of actin or *h*-caldesmon, after normalization to GAPDH (Fig. 4a). Western blot analysis of the non-denatured protein extracts revealed no significant change in the expression of the LC₁₇ isoforms from Fisher and Lewis rat tracheae (Fig. 4b). Interestingly, LC₁₇ isoform expression was similar for both the aorta and bladder in either of the strains. These results were corroborated by Coomassie staining of the urea-glycerol gels (not shown), as described previously [33].

A



B

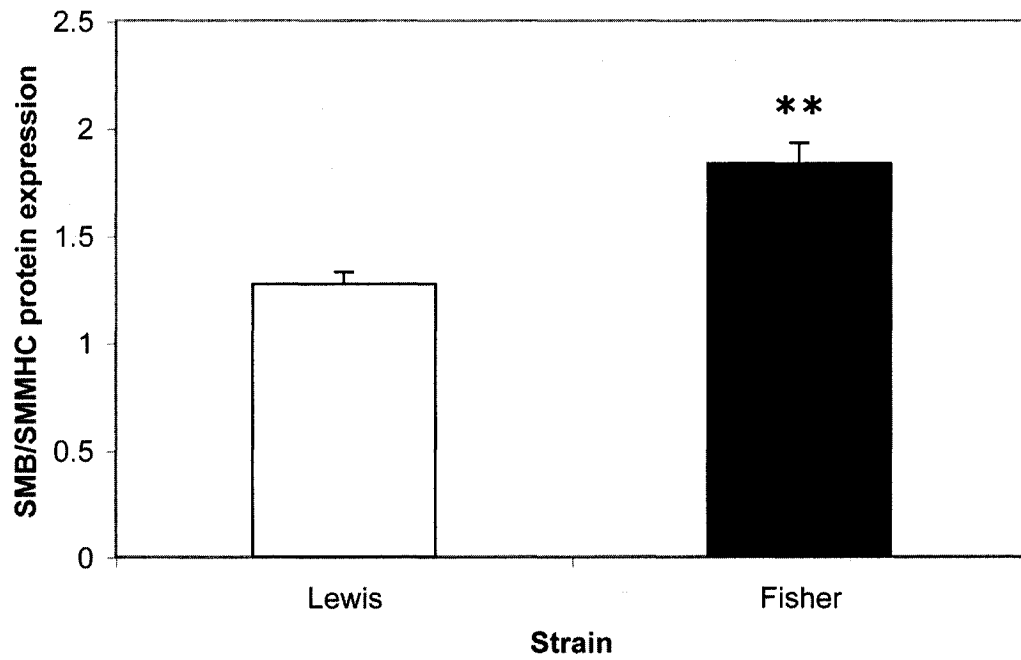
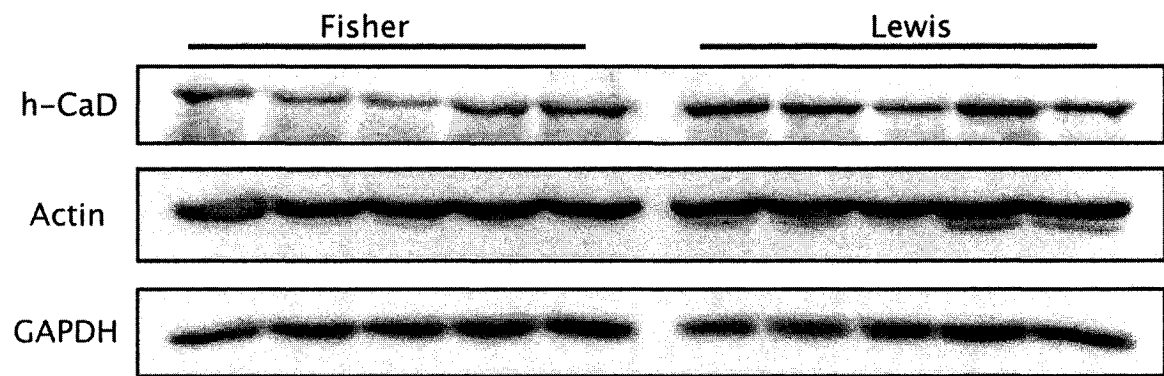


Figure 3: (+)insert isoform and total SMMHC protein content in Fisher and Lewis tracheae.

A. All samples from Fisher and Lewis tracheae were run together on the same gel, and probed for (+)insert isoform expression using a (+)insert-specific antibody. Membranes were then stripped, and probed with a general SMMHC antibody recognizing all isoforms. **B.** Analysis of the (+)insert isoform content, normalized to total SMMHC in the tracheae of Fisher and Lewis rats. $n=5$ for each strain, and Western blots were run in triplicate. The figure indicates the mean of the triplicate runs. $**p<0.01$

A



B

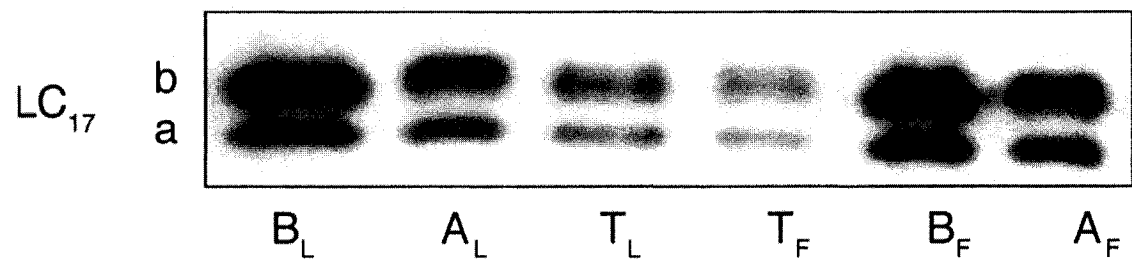


Figure 4: Western blots of other contractile proteins in smooth muscle from Fisher and Lewis rats.

A. Representative Western blot of *h*-CaD, actin, and GAPDH expression in Fisher and Lewis rat tracheae. Bars indicate which strain each of the different tracheal protein extract pertained to. *n*=5 for each strain. **B.** Representative Western blot of LC₁₇ isoforms transferred from urea-glycerol gels run in non-denaturing conditions. The following designations are used: B, bladder; A, aorta; and T, tracheae. The F and L subscripts designate the Fisher and Lewis strains, respectively. *n*=3 for each strain.

3.3. SEQUENCING THE COMPLETE (+)INSERT SMMHC cDNA

The sequence of the complete human (+)insert SMMHC (7 kb) was accomplished by RT-PCR using human bladder RNA. Compilation of the sequences obtained for the complete (+)insert SMMHC transcript revealed two isoforms of 6,882 and 6,921 bp (see supplementary information at <http://ajpcell.physiology.org/cgi/content/full/00244.2004/DC1>). Comparison with the available human (-)insert isoform sequence (GenBank accession no. NM-002474) revealed identical sequences, except for the 21 nucleotides coding for the 7-amino acid insert. This comparison also showed that the shorter mRNA product (6,882 bp) generates the longer SM1 protein and the longer mRNA product (6,921 bp) generates the shorter SM2 protein, because of the insertion of a short exon encoding a stop codon. Furthermore, there are no differences in the RNA encoding the carboxy-terminal amino acids, i.e., the (+) and (-)insert SM1 and the (+) and (-)insert SM2 isoforms. These human (+)insert SM1 and (+)insert SM2 SMMHC cDNA sequences are available on GenBank (accession nos. AY520816 and AY520817).

3.4. MYOSIN REGULATORY LIGHT CHAIN (LC₂₀)

PHOSPHORYLATION RESPONSE IN FISHER & LEWIS ANIMALS

A dose response curve was performed on tracheae from three Fisher and three Lewis animals, and 10^{-6} M MCh was chosen as a suitably sub-maximal stimulus (Fig. 5). The tracheal muscle strip tension generated at 30 s after a 10^{-6} M MCh challenge was greater for the Fisher (4.2 ± 0.8 mN) than for the Lewis rats (1.9 ± 0.4 mN) ($p < 0.05$) (Fig. 6a). The breakdown in the force response per tracheal segment is indicated in Fig. 6b. No difference in force response was observed for any of the segments except segment 2 ($p < 0.05$). The corresponding LC₂₀ phosphorylation level was assessed by quantifying in the same muscle strips, total LC₂₀ expression, baseline LC₂₀ phosphorylation level, as well as LC₂₀ phosphorylation level 30s after the MCh challenge. The total amount of LC₂₀ did not differ between Fisher (71.8 ± 1.6) and Lewis (66.3 ± 4.3) rats (Fig. 7b). Baseline phosphorylation level did not differ either between Fisher (17.3 ± 3.7) and Lewis (18.8 ± 5.9) rats (see L4 and F4 in Figs. 7a). However, the phosphorylation level at 30 s after MCh challenge was significantly greater for the Fisher (55.1 ± 6.4) than for the Lewis rats (41.4 ± 6.1) ($p < 0.01$) (Fig. 7b). Breakdown of the extent of LC₂₀ phosphorylation recruited per segment is indicated in Fig. 7c, though no difference was found for any of the segments.

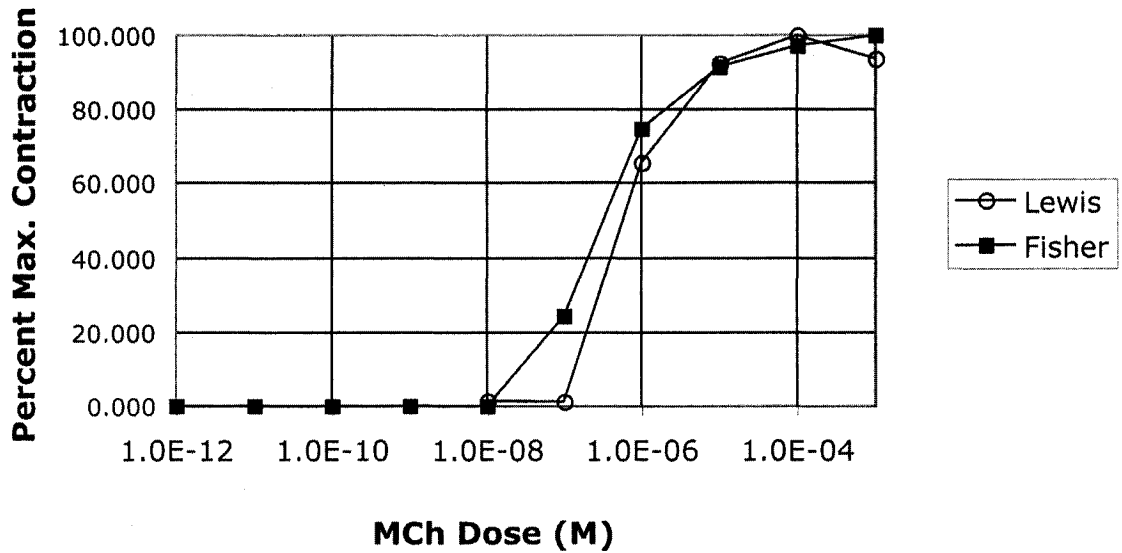
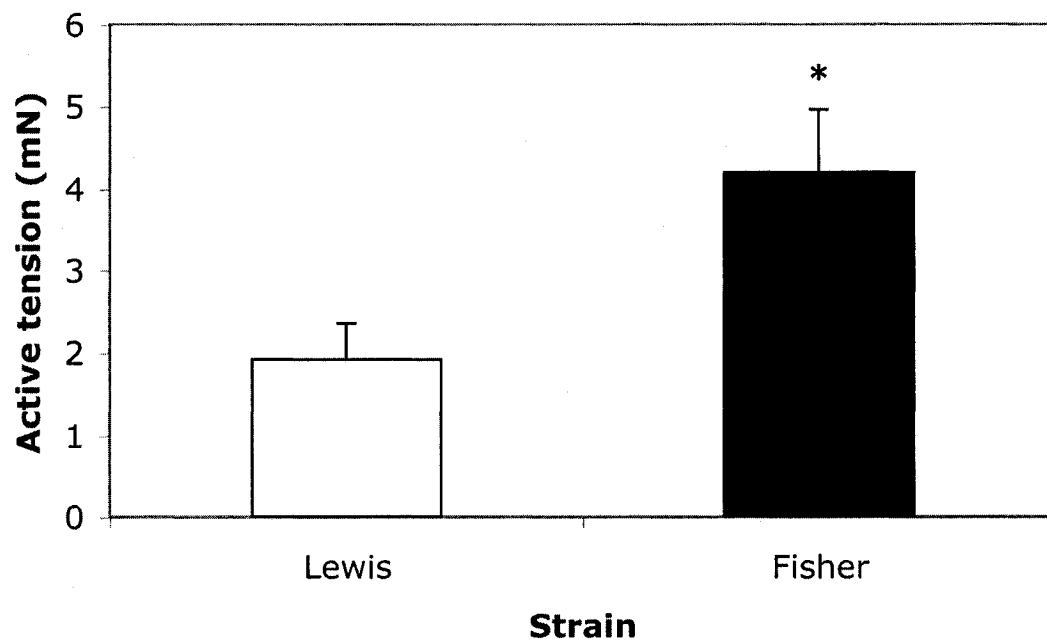


Figure 5: Dose-response curve of Fisher and Lewis tracheal smooth muscle strip to MCh.

A representative dose-response curve to MCh is shown for Fisher and Lewis tracheal strips stimulated *in vitro* in organ baths. A dose of methacholine of 10^{-6} M, which produces submaximal contraction in both Fisher and Lewis tracheal smooth muscle, was therefore chosen for the next experiments in order to avoid saturating the LC₂₀ phosphorylation signal.

A



B

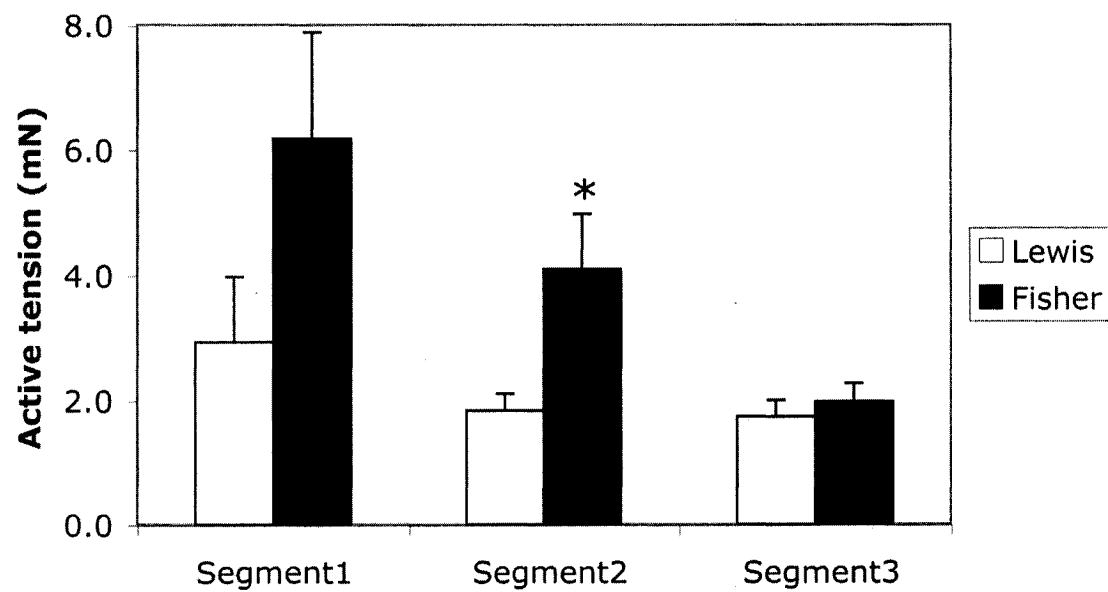
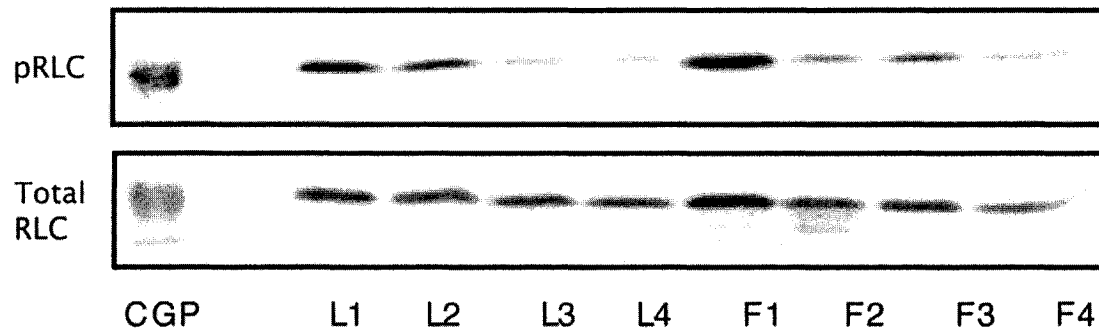


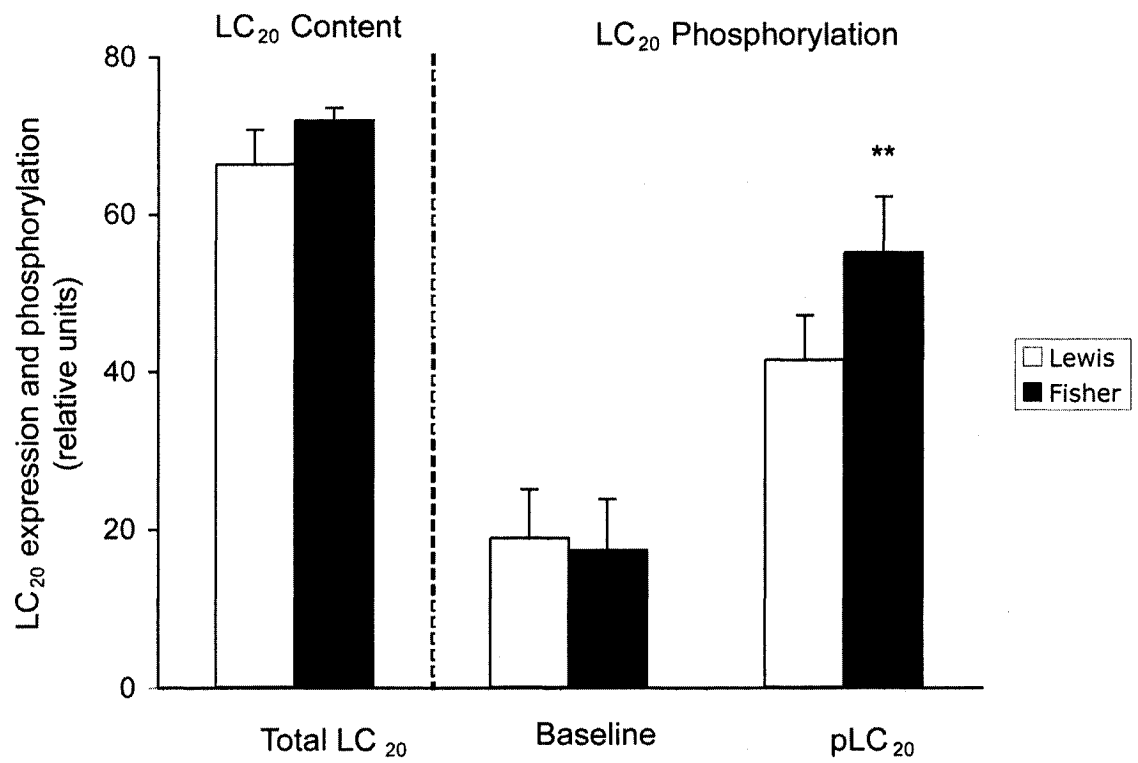
Figure 6: Isometric force response to submaximal stimulus of Fisher and Lewis tracheal strips.

A. Fisher and Lewis tracheal strips were stimulated *in vitro* with 10^{-6} M MCh, after which they were rapidly frozen for determining the extent of LC₂₀ phosphorylation. Shown in the figure is the average of the isometric force response elicited in the tracheae prior to removal for assessment of LC₂₀ phosphorylation. n=7 animals per strain. *p<0.05 **B.** Breakdown of the isometric force response from the most caudal segment (segment 1) to the most cranial segment stimulated (segment 3). *p<0.05

A



B



C

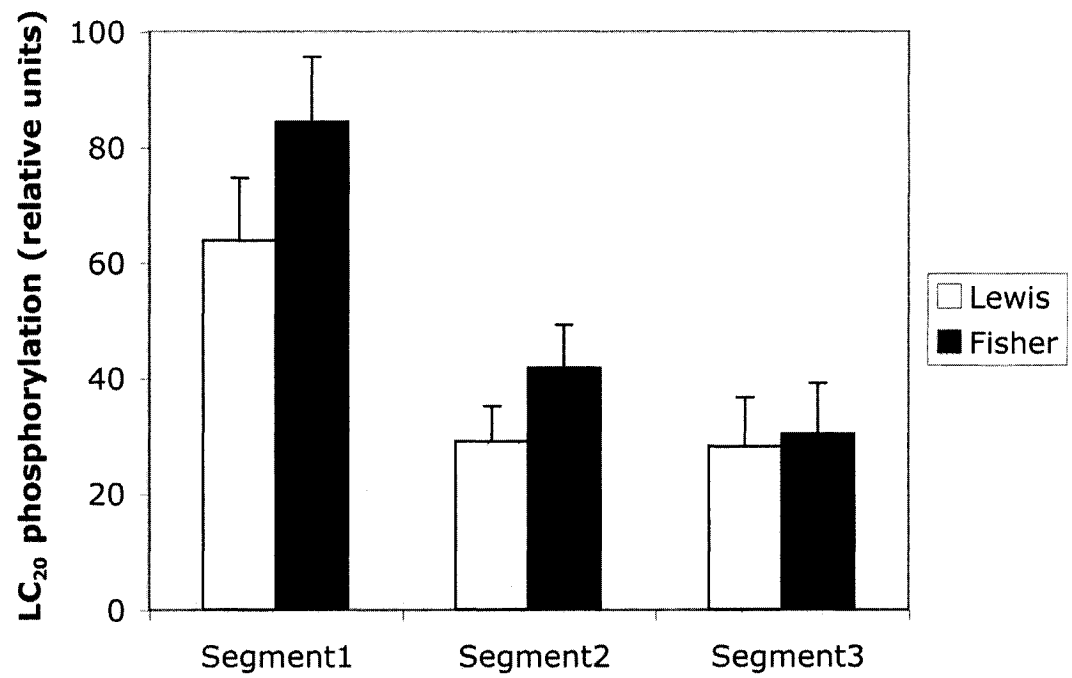


Figure 7: LC₂₀ phosphorylation mounted to submaximal stimulus with MCh in Fisher and Lewis tracheal strips.

A. Representative Western blot of Fisher and Lewis tracheal segments after stimulation with 10^{-6} M MCh. The various segments noted are labeled F or L, representing each strain, and the number (1-4) designates the order of the tracheal segments, from most caudal to most cranial. The upper blot is probed with an antibody specific to phosphorylated LC₂₀, whereas the lower blot is a probe of the same extracts with a non-specific LC₂₀ antibody. Segment 4 of both strains was not stimulated to provide an index of the degree of baseline LC₂₀ phosphorylation. CGP, chicken gizzard, phosphorylated (positive control). **B.** The total LC₂₀ expression, baseline LC₂₀ phosphorylation, and LC₂₀ phosphorylation was averaged for all stimulated segments of trachea and compared between the strains. $n=7$ animals per strain. $**p<0.01$ **C.** Breakdown of the extent of LC₂₀ phosphorylation among the different segments for the Fisher and Lewis rats. No statistical difference was found in the extent of LC₂₀ phosphorylation in any of the segments between the Fisher and Lewis rats.

3.5. THIOPHOSPHORYLATED FISHER & LEWIS TRACHEAL STRIPS

3.5.1. Intact muscle strip measurements

The optimal length of trachealis from 6 Fisher and 4 Lewis rats was first derived from the fitted active length-tension relations (Fig. 8). The fit of these graphs to the 4-parameter Weibull function was very good, with $R^2 > 0.999$ for all data sets. Interestingly, the optimal length of Fisher trachealis smooth muscle was found to be greater than in the Lewis, at 3.3 ± 0.1 mm and 2.3 ± 0.0 mm, respectively ($p < 0.01$). These data would suggest that Fisher animals possess larger tracheae, relative to the Lewis animals, and may reflect a difference in size of the entire bronchial tree.

Force-velocity data for Fisher and Lewis rats remain preliminary. An example force-velocity curve is indicated in Fig. 9. The y-intercept corresponds to the maximal velocity of shortening (V_{\max}) of that muscle. For the animals studied thus far, the average V_{\max} of Fisher rats was found to be 0.68 ± 0.12 l/s and Lewis was 0.44 ± 0.12 l/sec, though no significant difference was found for the data collected thus far (Fig. 10). The calculated differences in V_{\max} derived are similar to those previously reported in the literature, i.e. V_{\max} is 46% greater for the Fisher than for the Lewis rats [8].

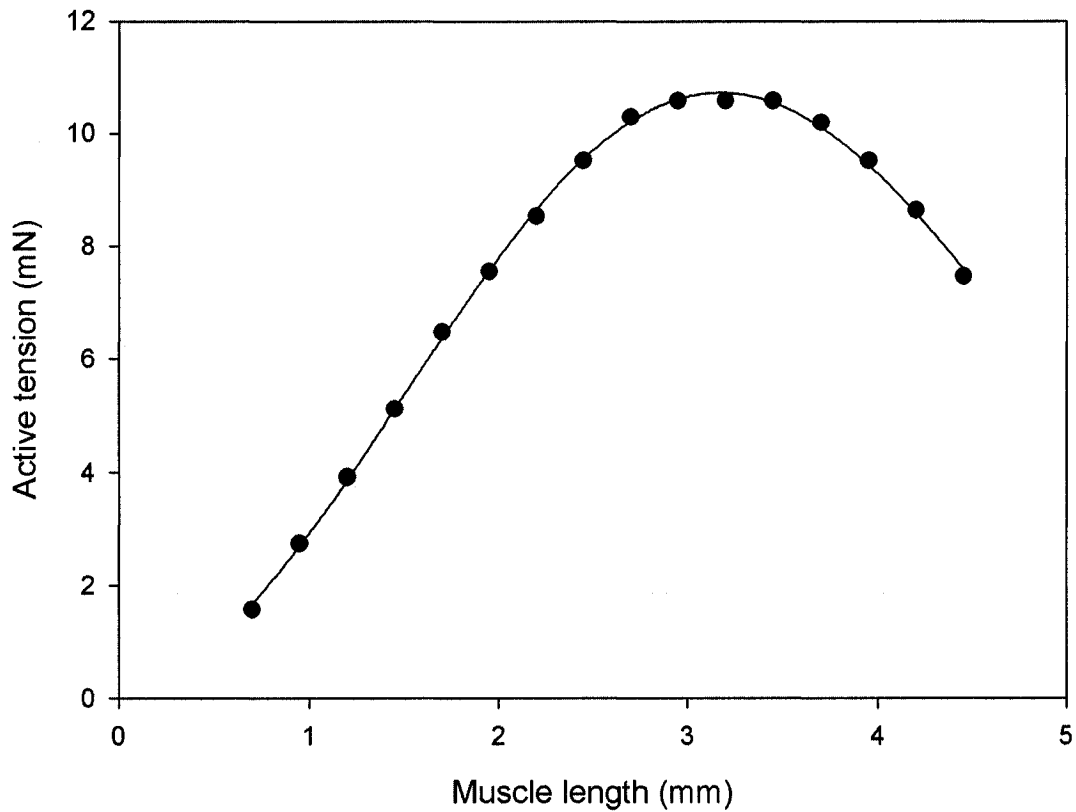


Figure 8: Representative active length-tension relation of trachealis.

An active length tension relation is shown taken from a Fisher animal. Between 7 and 16 points were collected to build the length-tension relations, depending on the relative stiffness of the particular muscle strip tested. The relation above is fitted to a 4-parameter Weibull function, and the peak of the curve is derived to obtain the optimal length (l_o) and maximal isometric force (P_o).

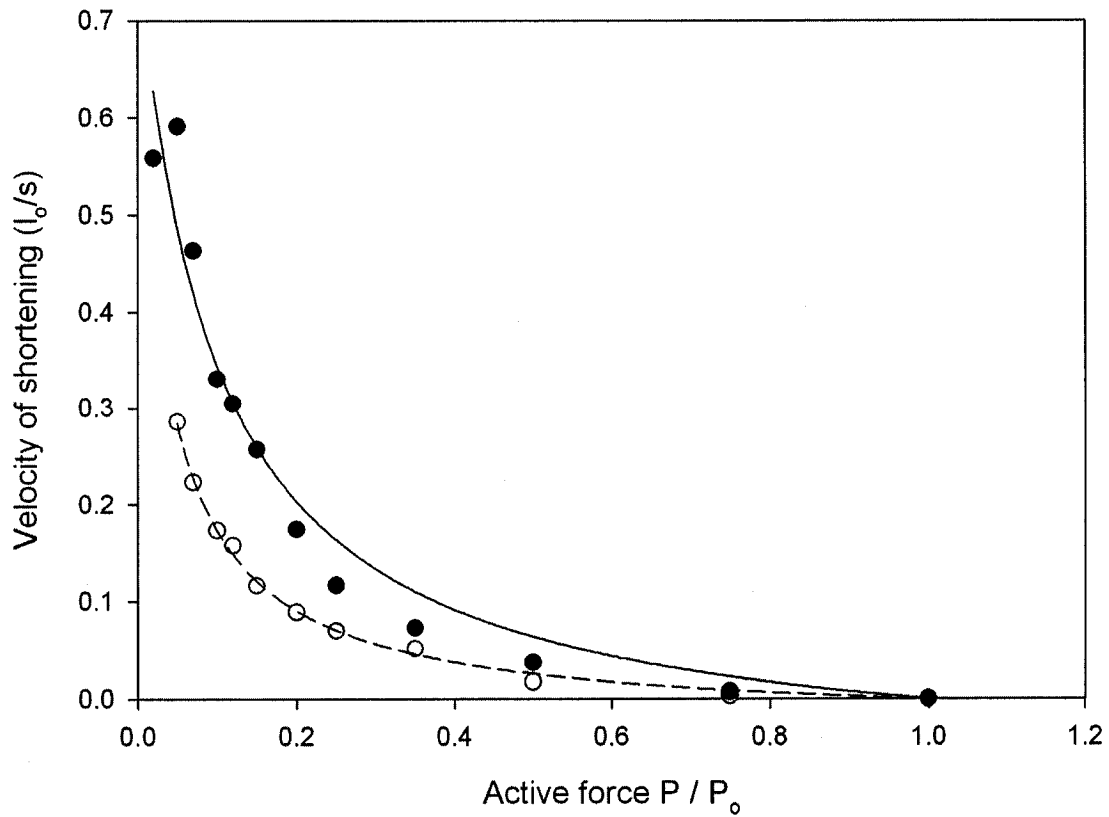


Figure 9: Representative force-velocity curves of Fisher and Lewis trachealis.

Representative force-velocity relationships from Fisher and Lewis rat tracheae are shown. Muscle length and active force developed have been corrected to the optimal length (l_0) and maximal isometric force (P_0), respectively, of that muscle. The curves are then fitted to Hill's equation [48] to derive the velocity of unloaded shortening (V_{max}). The open circles and dashed line denote data from a Lewis trachea, whereas the shaded circle and solid line are from a Fisher trachea.

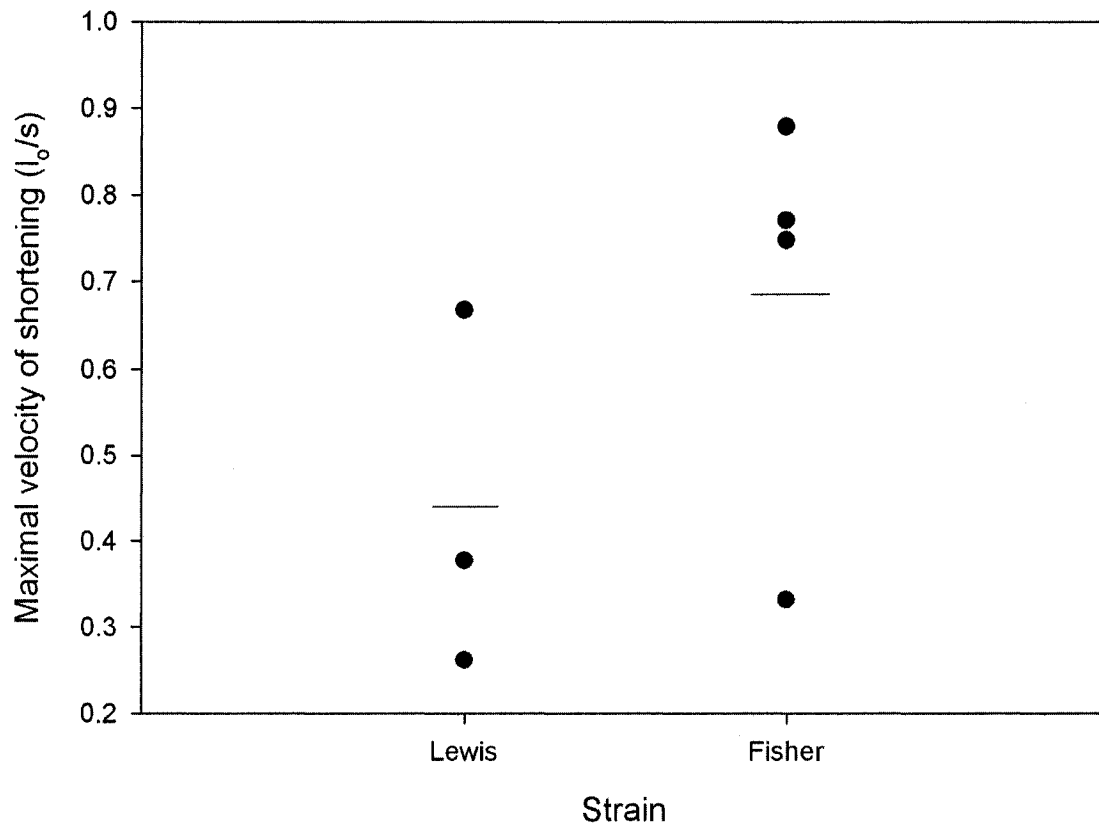


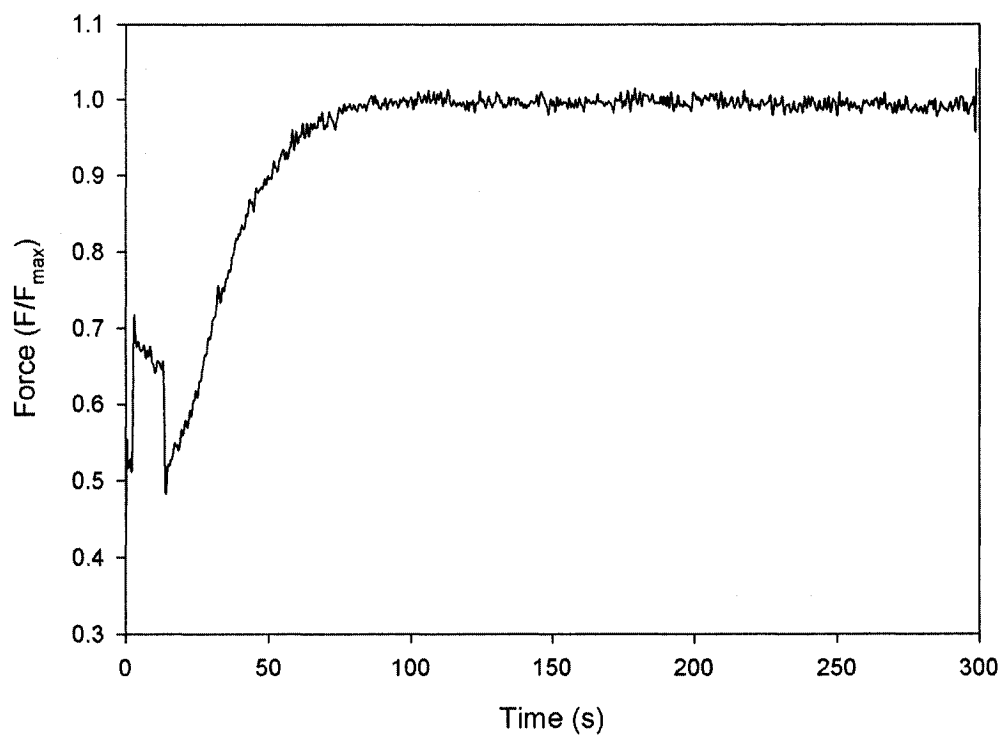
Figure 10: Velocity of maximal shortening for Fisher and Lewis tracheal strips (preliminary).

A series of quick-releases at different loads were performed on tracheal strips stimulated by EFS. These data were then plotted and fit to Hill's equation. The maximal velocity of smooth muscle shortening was extrapolated to velocity of shortening at zero load on the muscle. Horizontal bar designates mean for each strain.

3.5.2. Muscle thiophosphorylation

Preliminary data collected from the thiophosphorylation experiments suggest that there are differences in the contractility between Fisher and Lewis tracheal smooth muscle under conditions of maximal LC₂₀ activation. Viability of the β -escin – permeabilized smooth muscle was verified by stimulating the muscle with 5 μ M CaM at pCa 4.5. Contraction of thiophosphorylated strips was established by changing the nucleotide-free Rigor solution to relaxing solution (containing ATP). Contraction of thiophosphorylated muscles to the relaxing solution usually occurred on a faster time course compared to permeabilized, non-thiophosphorylated muscle strips. Representative traces of force response to ATP are shown for thiophosphorylated Fisher and Lewis trachea (Fig. 11). The nature of the force response suggests that there may be differences in the time course of force development between the two trachea. However, high variability in the data set suggest that other limiting factors, such as the rate of ATP diffusion into the muscle cells, may be affecting that rate at which force develops. Thus, thinner strips will have to be used along with more sensitive force transducers.

A



B

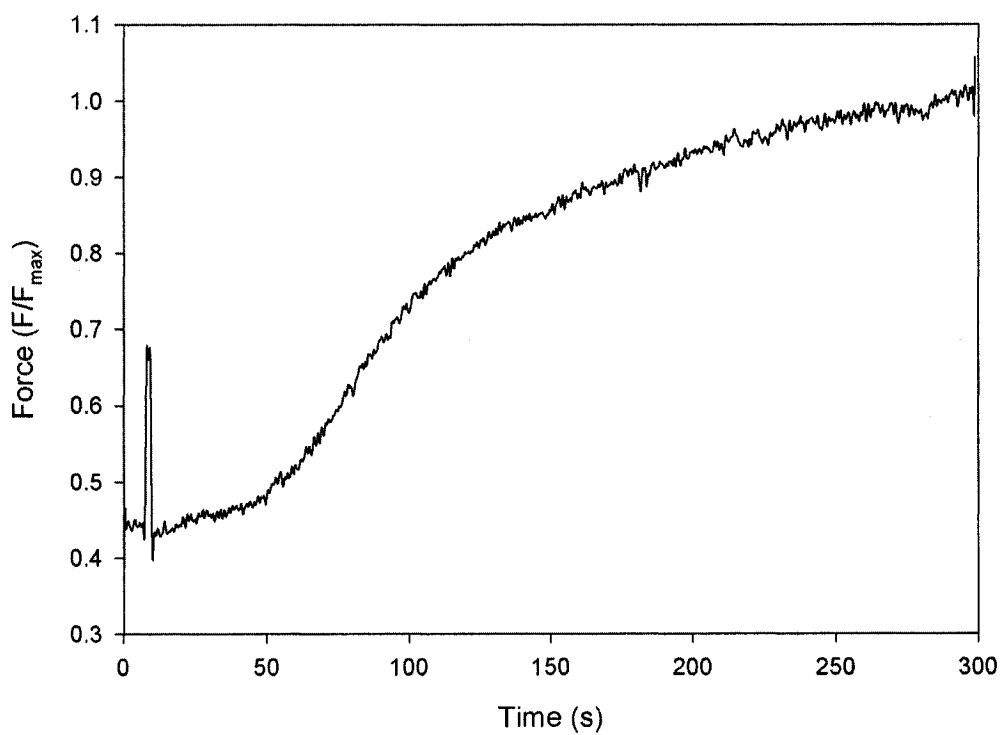


Figure 11: Force development of thiophosphorylated tracheal strips from Fisher and Lewis rats.

Tracheal strips were induced to contract by transferring from a nucleotide-free bath to a Ca^{2+} -free solution containing Na_2ATP . Force (F/F_{max}) is the measured force normalized to the maximal isometric force. **A.** Force development curve for thiophosphorylated Fisher tracheal strip. **B.** Force development curve for thiophosphorylated Lewis tracheal strip.

CHAPTER IV. DISCUSSION

Considerable advances have been made into the understanding and management of asthma. However, many of the findings to date on asthma have been impinged upon by the complex and heterogeneous nature of its etiology and pathophysiology. This has made it difficult to establish consensus on the specific characteristics of asthma, such as airway remodeling and altered smooth muscle force development. Models of the various characteristics of asthma, such as innate or acquired airway hyperresponsiveness have proven an invaluable tool in providing indirect insight into the various factors underlying abnormal reactivity of the airways. These models are particularly useful in that they not only illustrate the pathophysiology of the disorder, but also can be used to study genetic factors predisposing to the development of airway hyperresponsiveness [28].

Airway smooth muscle contractility has long been suspected to play a key role in the symptomatology of airway hyperresponsiveness, and this was first demonstrated in sensitized dogs [3]. In humans, the significance of a hypercontractile airway smooth muscle is evident in that β -agonists are routinely used to alleviate acute episodes of bronchoconstriction, as suffered during an asthmatic attack. The Fisher and Lewis rat model of airway hyperresponsiveness is a well-established model, characterized by differences in airway mechanics to bronchoconstrictive challenge [35] and airway smooth muscle contractility [8,56]. In all these various models of

airway hyperresponsiveness, it is becoming increasingly recognized that velocity of shortening is the parameter of choice to detect differences in contractility compared to normal ASM. Consistent findings in sensitized ASM from humans [81,88] suggest that velocity of shortening is the parameter of choice for determining differences in airway smooth muscle contractility in asthma [11].

Differences were found in the expression of SMMHC isoforms in the airways of the Fisher and Lewis rats. Specifically, a significantly greater content of the (+)insert SMMHC isoform was found in the hyperresponsive Fisher animal compared to the Lewis strain. This difference was unique to the airways; expression of the (+)insert isoform in the aorta or bladder was similar between the strains. Moreover, the discrepancy in SMMHC isoform expression was not accompanied by any difference in the expression of total SMMHC, *h*-caldesmon, actin, or LC₁₇ isoforms.

In addition to the lack of differences in tracheal LC₁₇ isoforms between Fisher and Lewis rats, expression of these isoforms did not differ between the aorta and bladder of either strain. This finding was surprising, given the link that various studies have shown between SMMHC isoform expression and expression of the LC₁₇ isoforms [29,104,116]. However, others have also reported no difference in LC₁₇ isoforms among several smooth muscle tissues [106], while others did not find any relationship between expression of the LC₁₇ isoforms and smooth muscle contractility [33,103]. Moreover, what functional difference the LC₁₇ isoforms may have remains

unclear. Switching the expression of these isoforms on myosin did not show any effects on ATPase activity or *in vitro* actin motility [100], prompting Rovner and co-workers to suggest that, apart from LC₂₀ phosphorylation, the 7 amino acid insert remains the principal determinant of the kinetics of SMMHC.

Previous results had suggested that the (+)insert isoform does not exist in humans, minimizing the significance of studies on the SMMHC isoforms [81]. However, using primer sequences designed from the published human (-)insert SMMHC, the human (+)insert SM1 and SM2 SMMHC isoforms were identified and sequenced. These findings are particularly interesting in that studies showing changes in SMMHC isoform expression during development, hormonal levels, and pathophysiology are likely to hold true for humans. Moreover, other work done in our lab quantifying the human isoforms from airway biopsies found a more than 2-fold greater content of the fast, (+)insert isoform in asthmatic compared to normal airways [74]. This increased expression accompanied only a modest increase in the expression of total SMMHC. The expression of the (+)insert isoform has also been quantified for a panel of various human smooth muscle tissues [73].

In this study, we chose to use the trachea as a model of the airways of the Fisher and Lewis rats to facilitate comparisons with the majority of other studies on airway hyperresponsiveness, including those on the Fisher and Lewis rats, which utilize tracheal smooth muscle. For technical reasons, tracheal smooth muscle is easier to use for the mechanical measurements as well as provide results with greater con-

sistency. While the trachealis can never provide an exact index of the function of the smooth muscle of the lower airways, tracheal smooth muscle is routinely taken to be representative of the mechanical properties of ASM in peripheral airways [3,56]. In comparisons, whatever differences found for tracheal smooth muscle between strains are likely to be reflected in the more peripheral airways, thus corroborating with the differences in pulmonary mechanics previously reported [35].

The correlations between (+)insert SMMHC isoform content and smooth muscle velocity of shortening in other smooth muscle tissues [65] suggest that the greater content of the (+)insert isoform in the ASM of Fisher airways compared to that of Lewis airways likely plays a role in conferring the greater velocity of shortening that has been previously characterized for this ASM [8]. Differences in SMMHC isoform expression are also likely to accompany the increased velocity of ASM shortening that has been reported in other models of airway hyperresponsiveness [36,52,59]. The likely role of the SMMHC isoforms to the enhanced ASM contractility of hyperresponsive airways is further substantiated in previous reports on an increased ATPase activity in the ASM of sensitized dogs that has been suggested to determine the enhanced velocity of shortening characterized for this ASM [98]. However, differences in SMMHC isoform content are not the only factors that can mediate an enhanced ATPase activity of the ASM from hyperresponsive airways.

In this thesis, an organ-specific difference in SMMHC isoform expression was found for the trachea, whereas no change was seen in the aorta or bladder. Similarly,

others have reported a difference in expression of (+)insert isoform expression in cardiac vessels that was not seen in other smooth muscle organs. Specifically, a lower expression of the (+)insert SMMHC isoform was found in cardiac precapillary arterioles from a spontaneously hypertensive inbred rat strain compared to the control strain [129]. However, no work on the contractility of the muscle from the vessels studied has been reported, so the functional significance of this differential SMMHC isoform expression remains unknown. A related study on hypertension in inbred rats gave further evidence suggesting that the expression of the SMMHC isoforms in the cardiac vessels is genetically determined and does not change if hypertension is induced [128]. These data suggest that the expression of SMMHC isoforms in various smooth muscle organs is genetically determined. Thus, a particular expression pattern of these isoforms may wholly or in part determine the mechanical properties of a particular smooth muscle, and thereby have an effect on the functioning of the respective organ.

Another train of thought is that the signaling response determining the extent of LC₂₀ activation is enhanced in such airways. One study has reported an increased content of MLCK in sensitized airways, leading to a greater recruitment of myosin for contraction [58]. Moreover, in the Fisher and Lewis rats, a greater Ca²⁺ mobilization has been shown in Fisher ASM in response to stimulus, a phenomenon upstream of the involvement of MLCK [118]. This enhanced Ca²⁺ mobilization response is reflected by a greater amount of LC₂₀ phosphorylation in response to a

submaximal stimulus. These data provide the direct link between previous work describing an enhanced calcium due to a greater inositol (1,4,5)-triphosphate mobilization response of ASM myocytes from this model [118,119] to contractility. In a follow-up study, Tao and coworkers further went on to suggest that variations in the regulation of protein kinase C between the Fisher and Lewis rats are likely responsible for the differences in Ca^{2+} mobilization that have been reported previously in these rat strains [117]. These results demonstrate that the extent of LC_{20} activation, and thus myosin recruitment, is intrinsically determined and under genetic control.

Differences in contractility and myosin activation were also noted along the trachea of both Fisher and Lewis rats, showing a trend towards increasing isometric force output and extent of LC_{20} phosphorylation going from the carina towards the bronchial bifurcation. These regional differences in the mechanical properties of the trachea have also been observed by others [40], and these differences appear are paralleled by differences in the extent of LC_{20} phosphorylation. While a trend toward greater contractility and LC_{20} phosphorylation in the trachea towards the bronchial bifurcation were seen in both strains, the trend was more pronounced in the Fisher animal. It would be interesting to see if SMMHC isoform expression changes in a similar way. However, whole tracheae, rather than segments, were needed to examine SMMHC isoform expression because of the limited amounts of total myosin that can be extracted from this small muscle with current protocols available.

In light of the greater extent of LC₂₀ phosphorylation for a given stimulus in Fisher compared to Lewis ASM, it remains to be seen how the differences in SMMHC isoforms directly affect the contractility of the muscle. By examining the maximal velocity of muscle shortening of thiophosphorylated ASM strips from Fisher and Lewis rats, it is possible to dissect out potential differences that might remain in the mechanics of the molecular contractile machinery of this smooth muscle. In thiophosphorylation, the muscle signaling machinery has been bypassed, and therefore any differences in force development between thiophosphorylated muscles would reflect differences at the level of the contractile filaments, specifically myosin. Already, this has been used to demonstrate a 7-fold difference in the velocity of phasic and tonic smooth muscles [83]. Another study using this method demonstrated that a decrease in SMMHC isoform expression in hypertrophied intestinal smooth muscle was accompanied by a reduction in the velocity of shortening [76].

This specific project has not yet been finished, and optimization of the protocol as well as processing of a larger sample of animals remains to be done. Successful permeabilization and thiophosphorylation have thus far been performed on one animal from each strain, and the results point to a difference in the rate of force development of the thiophosphorylated fibers. From preliminary experiments, the differences in V_{\max} extrapolated for intact Fisher and Lewis muscle strips correspond well with those that have been reported previously [8]. More experiments will be performed to determine if the differences in velocity of shortening are preserved af-

ter thiophosphorylation, which would support the involvement of the SMMHC isoforms. If not, it would be concluded that the differences in V_{\max} are exclusively in the domain of regulation by LC_{20} activation.

Given the strong correlations that have been previously reported in the literature concerning SMMHC isoform expression and smooth muscle contractility [6,29,44,84,104], it would seem quite plausible that the increased (+)insert SMMHC isoform expression plays a role in mediating the enhanced contractility of the hyper-responsive Fisher rat. This would have potentially significant implications in elucidating the pathophysiology of asthma. While asthma is a disorder generally characterized by inflammation and airway hyperresponsiveness, it has been shown that the development of airway hyperresponsiveness is inherited distinctly from atopy, based on studies of family pedigrees and twins [78]. Similar data have also been obtained from experimental models using inbred animal strains [36]. The difference in airway response between the Fisher and Lewis rats is of intrinsic origins, with no concomitant inflammation occurring in the airways [85]. We have found increased expression of the (+)insert SMMHC isoform along with a greater LC_{20} phosphorylation response in hyperresponsive Fisher ASM compared to the Lewis strain. These results may be indicative of a complement of differences in smooth muscle phenotype that combine to lead to a hypercontractile ASM. This would be consistent with the theory of asthma as a disorder of polygenetic origins [9]. The results obtained in our lab of greater (+)insert isoform expression in asthmatic airway biopsies [74] suggest

that greater (+)insert SMMHC isoform expression and LC₂₀ phosphorylation may represent predisposing characteristics that can be found in the general population that lie dormant until additional factors induce the onset of asthma. Alternatively, a greater (+)insert SMMHC isoform expression and LC₂₀ phosphorylation may on their own incite the development of airway hyperresponsiveness and asthma.

β-agonists are commonly used to relax the ASM and alleviate acute episodes of asthma. However, asthma is a chronic disorder characterized by recurrent airway narrowing, due to the hypercontractile nature of the underlying ASM. A natural strategy to manage this problem would thus be to reduce its contractility. As the SMMHC isoforms are likely implicated in the manifestation of such hypercontractility, strategies to reduce the expression of fast SMMHC isoform would naturally be a good solution for the management of hyperresponsive ASM. Expression of the SMMHC isoform has been shown to change under various conditions, such as cell culture [4]. Various hormones have also been shown to be capable of modulating the expression of SMMHC isoforms [16,77]. However, the mechanism by which the alternative splicing process that generates the different SMMHC isoforms remains poorly understood. Ultimately, the mechanism by which SMMHC mRNA splicing is regulated may also be related to the process that determines the overall contractility of the smooth muscle cell. In the Fisher airways, a greater expression of the faster SMMHC isoform was found but no significant differences were observed in the expression of other contractile proteins. This would suggest that switches in SMMHC

isoform expression are thus far the best indicators of muscle contractility as opposed to other contractile proteins associated with the phasic / tonic dichotomy, such as the LC₁₇ isoforms, actin, and *h*-caldesmon. Since myosin is the mechanoenzyme directly responsible for effecting contraction, its isoform expression would naturally be the best indicator of changes in contractility to the same muscle tissue.

To conclude, differences in SMMHC isoform expression and LC₂₀ phosphorylation were found in the ASM of the Fisher and Lewis rats. Given that these differences were found in this innate model of airway hyperresponsiveness would suggest that airway smooth muscle contractility is genetically determined by expression of SMMHC isoforms as well as the extent of myosin activation. Future studies on these findings could provide insight into the development of airway hyperresponsiveness, as well as factors that can predispose an individual or animal to develop asthma. The next step to follow this work is to elucidate the mechanism of alternative splicing that determines the expression of the SMMHC isoforms will improve our understanding of the mechanism that governs and/or alters smooth muscle contractility. A better insight of how smooth muscle contractility is determined will help to provide identify targets for the management of pathological abnormalities in smooth muscle contractility.

FINAL CONCLUSION AND SUMMARY

The pathophysiology of airway hyperresponsiveness remains rather nebulous. I have demonstrated that the intrinsic properties of the ASM are distinct in a rat model of airway hyperresponsiveness. Specifically, a difference in the expression of SMMHC isoforms was found for hyperresponsive ASM, with no accompanying changes in expression of other contractile proteins, and no changes in SMMHC isoform expression in other smooth muscle tissues. There is also a concomitant difference in the extent of myosin activation by LC₂₀ phosphorylation. The specific role of this expression pattern of the SMMHC isoforms remains to be determined by velocity of shortening measurements of thiophosphorylated muscle tissues. However, the recent findings in our lab of a difference in SMMHC isoform expression from airway biopsies from asthmatic and normal individuals [74] suggests that they may play a significant role in abnormal ASM contractility, and warrant further study. In conclusion, since my findings of a difference in SMMHC isoform expression are based on a model of intrinsic airway hyperresponsiveness with no associated inflammation, it would suggest that differences in SMMHC isoform expression might lead to a predisposition towards the development of airway hyperresponsiveness by enhancing the contractility of ASM.

REFERENCES

1. ALBERTS B, BRAY D, LEWIS J, RAFF M, ROBERTS K, WATSON JD. (1989). *Molecular Biology of the Cell*.
2. AMRANI Y, PANETTIERI RA. (2003). Airway smooth muscle: contraction and beyond. *Int J Biochem Cell Biol*; **35(3)**:272-276.
3. ANTONISSEN LA, MITCHELL RW, KROEGER EA, KEPRON W, TSE KS, STEPHENS NL. (1979). Mechanical alterations of airway smooth muscle in a canine asthmatic model. *J Appl Physiol*; **46(4)**:681-687.
4. ARAFAT HA, KIM GS, DISANTO ME, WEIN AJ, CHACKO S. (2001). Heterogeneity of bladder myocytes in vitro: modulation of myosin isoform expression. *Tissue Cell*; **33(3)**:219-232.
5. ARMOUR CL, BLACK JL, BEREND N, WOOLCOCK AJ. (1984). The relationship between bronchial hyperresponsiveness to methacholine and airway smooth muscle structure and reactivity. *Respir Physiol*; **58(2)**:223-233.
6. BABU GJ, LOUKIANOV E, LOUKIANOVA T, et al. (2001). Loss of SM-B myosin affects muscle shortening velocity and maximal force development. *Nat Cell Biol*; **3(11)**:1025-1029.

7. BABU GJ, WARSHAW DM, PERIASAMY M. (2000). Smooth muscle myosin heavy chain isoforms and their role in muscle physiology. *Microsc Res Tech*; **50(6)**:532-540.
8. BLANC FX, COIRAULT C, SALMERON S, CHEMLA D, LECARPENTIER Y. (2003). Mechanics and crossbridge kinetics of tracheal smooth muscle in two inbred rat strains. *Eur Respir J*; **22(2)**:227-234.
9. BLUMENTHAL JB, BLUMENTHAL MN. (2002). Genetics of asthma. *Med Clin North Am*; **86(5)**:937-950.
10. BRACKEL HJ, PEDERSEN OF, MULDER PG, OVERBEEK SE, KERREBIJN KF, BOGAARD JM. (2000). Central airways behave more stiffly during forced expiration in patients with asthma. *Am J Respir Crit Care Med*; **162(3 Pt 1)**:896-904.
11. BRAMLEY AM, THOMSON RJ, ROBERTS CR, SCHELLENBERG RR. (1994). Hypothesis: excessive bronchoconstriction in asthma is due to decreased airway elastance. *Eur Respir J*; **7(2)**:337-341.
12. BROWN RH, MITZNER W. (1998). The myth of maximal airway responsiveness in vivo. *J Appl Physiol*; **85(6)**:2012-2017.

13. BROWN RH, SCICHILONE N, MUDGE B, DIEMER FB, PERMUTT S, TOGIAS A. (2001). High-resolution computed tomographic evaluation of airway distensibility and the effects of lung inflation on airway caliber in healthy subjects and individuals with asthma. *Am J Respir Crit Care Med*; **163**(4):994-1001.
14. BRUSASCO V, CRIMI E, BARISONE G, SPANEVELLO A, RODARTE JR, PELLEGRINO R. (1999). Airway responsiveness to methacholine: effects of deep inhalations and airway inflammation. *J Appl Physiol*; **87**(2):567-573.
15. BURNS GP, GIBSON GJ. (1998). Airway hyperresponsiveness in asthma. Not just a problem of smooth muscle relaxation with inspiration. *Am J Respir Crit Care Med*; **158**(1):203-206.
16. CALOVINI T, HAASE H, MORANO I. (1995). Steroid-hormone regulation of myosin subunit expression in smooth and cardiac muscle. *J Cell Biochem*; **59**(1):69-78.
17. CHACKO S, DISANTO M, MENON C, ZHENG Y, HYPOLITE J, WEIN AJ. (1999). Contractile protein changes in urinary bladder smooth muscle following outlet obstruction. *Adv Exp Med Biol*; **462**:137-153.
18. CHANG S, HYPOLITE JA, ZDERIC SA, WEIN AJ, CHACKO S, DISANTO ME. (2002). Enhanced force generation by corpus cavernosum smooth muscle in rabbits with partial bladder outlet obstruction. *J Urol*; **167**(6):2636-2644.

19. CHEN Y, JOHANSEN H. (2004). Health Reports: Asthma. *Statistics Canada*; **16(2)**
20. CHITANO P, COX CM, MURPHY TM. (2002). Relaxation of guinea pig trachealis during electrical field stimulation increases with age. *J Appl Physiol*; **92(5)**:1835-1842.
21. CHITANO P, MURPHY TM. (2003). Maturational changes in airway smooth muscle shortening and relaxation. Implications for asthma. *Respir Physiol Neurobiol*; **137(2-3)**:347-359.
22. CHITANO P, WANG J, COX CM, STEPHENS NL, MURPHY TM. (2000). Different ontogeny of rate of force generation and shortening velocity in guinea pig trachealis. *J Appl Physiol*; **88(4)**:1338-1345.
23. CHUNG KF. (1986). Role of inflammation in the hyperreactivity of the airways in asthma. *Thorax*; **41(9)**:657-662.
24. CLIFFORD RD, PUGSLEY A, RADFORD M, HOLGATE ST. (1987). Symptoms, atopy, and bronchial response to methacholine in parents with asthma and their children. *Arch Dis Child*; **62(1)**:66-73.
25. COCKCROFT DW, KILLIAN DN, MELLON JJ, HARGREAVE FE. (1977). Bronchial reactivity to inhaled histamine: a method and clinical survey. *Clin Allergy*; **7(3)**:235-243.

26. DANDURAND RJ, XU LJ, MARTIN JG, EIDELMAN DH. (1993). Airway-parenchymal interdependence and bronchial responsiveness in two highly inbred rat strains. *J Appl Physiol*; **74**(2):538-544.
27. DE JONGSTE JC, MONS H, BONTA IL, KERREBIJN KF. (1987). In vitro responses of airways from an asthmatic patient. *Eur J Respir Dis*; **71**(1):23-29.
28. DE SANCTIS GT, DRAZEN JM. (1997). Genetics of native airway responsiveness in mice. *Am J Respir Crit Care Med*; **156**(4 Pt 2):S82-8.
29. DISANTO ME, STEIN R, CHANG S, et al. (2003). Alteration in expression of myosin isoforms in detrusor smooth muscle following bladder outlet obstruction. *Am J Physiol Cell Physiol*; **285**(6):C1397-410.
30. DUGUET A, BIYAH K, MINSHALL E, et al. (2000). Bronchial responsiveness among inbred mouse strains. Role of airway smooth-muscle shortening velocity. *Am J Respir Crit Care Med*; **161**(3 Pt 1):839-848.
31. DULIN NO, FERNANDES DJ, DOWELL M, et al. (2003). What evidence implicates airway smooth muscle in the cause of BHR? *Clin Rev Allergy Immunol*; **24**(1):73-84.
32. EBINA M, TAKAHASHI T, CHIBA T, MOTOMIYA M. (1993). Cellular hypertrophy and hyperplasia of airway smooth muscles underlying bronchial asthma. A 3-D morphometric study. *Am Rev Respir Dis*; **148**(3):720-726.

33. EDDINGER TJ, KORWEK AA, MEER DP, SHERWOOD JJ. (2000). Expression of smooth muscle myosin light chain 17 and unloaded shortening in single smooth muscle cells. *Am J Physiol Cell Physiol*; **278(6)**:C1133-42.
34. EDDINGER TJ, MEER DP. (2001). Single rabbit stomach smooth muscle cell myosin heavy chain SMB expression and shortening velocity. *Am J Physiol Cell Physiol*; **280(2)**:C309-16.
35. EIDELMAN DH, DIMARIA GU, BELLOFIORE S, WANG NS, GUTTMANN RD, MARTIN JG. (1991). Strain-related differences in airway smooth muscle and airway responsiveness in the rat. *Am Rev Respir Dis*; **144(4)**:792-796.
36. FAN T, YANG M, HALAYKO A, MOHAPATRA SS, STEPHENS NL. (1997). Airway responsiveness in two inbred strains of mouse disparate in IgE and IL-4 production. *Am J Respir Cell Mol Biol*; **17(2)**:156-163.
37. FERNANDES DJ, MITCHELL RW, LAKSER O, DOWELL M, STEWART AG, SOLWAY J. (2003). Do inflammatory mediators influence the contribution of airway smooth muscle contraction to airway hyperresponsiveness in asthma? *J Appl Physiol*; **95(2)**:844-853.
38. FISH JE, ANKIN MG, KELLY JF, PETERMAN VI. (1981). Regulation of bronchomotor tone by lung inflation in asthmatic and nonasthmatic subjects. *J Appl Physiol*; **50(5)**:1079-1086.

39. FLAVAHAN NA, AARHUS LL, RIMELE TJ, VANHOUTTE PM. (1985). Respiratory epithelium inhibits bronchial smooth muscle tone. *J Appl Physiol*; **58(3)**:834-838.
40. FLORIO C, STYHLER A, HEISLER S, MARTIN JG. (1996). Mechanical responses of tracheal tissue in vitro: dependence on the tissue preparation employed and relationship to smooth muscle content. *Pulm Pharmacol*; **9(3)**:157-166.
41. FREDBERG JJ. (2004). Bronchospasm and its biophysical basis in airway smooth muscle. *Respir Res*; **5(1)**:2.
42. FREDBERG JJ, INOUE D, MILLER B, et al. (1997). Airway smooth muscle, tidal stretches, and dynamically determined contractile states. *Am J Respir Crit Care Med*; **156(6)**:1752-1759.
43. FUGLSANG A, KHROMOV A, TOROK K, SOMLYO AV, SOMLYO AP. (1993). Flash photolysis studies of relaxation and cross-bridge detachment: higher sensitivity of tonic than phasic smooth muscle to MgADP. *J Muscle Res Cell Motil*; **14(6)**:666-677.
44. GOMES CM, DISANTO ME, HORAN P, LEVIN RM, WEIN AJ, CHACKO S. (2000). Improved contractility of obstructed bladders after Tadenan treatment is associated with reversal of altered myosin isoform expression. *J Urol*; **163(6)**:2008-2013.

45. GUNST SJ, MEISS RA, WU MF, ROWE M. (1995). Mechanisms for the mechanical plasticity of tracheal smooth muscle. *Am J Physiol*; **268**(5 Pt 1):C1267-76.
46. HAMADA Y, YANAGISAWA M, KATSURAGAWA Y, et al. (1990). Distinct vascular and intestinal smooth muscle myosin heavy chain mRNAs are encoded by a single-copy gene in the chicken. *Biochem Biophys Res Commun*; **170**(1):53-58.
47. HELPER DJ, LASH JA, HATHAWAY DR. (1988). Distribution of isoelectric variants of the 17,000-dalton myosin light chain in mammalian smooth muscle. *J Biol Chem*; **263**(30):15748-15753.
48. HILL AV. (1938). The heat of shortening and the dynamic constants of muscle. *Proc R Soc Lond B Biol Sci*; **126** (843):136-195.
49. HORIUTI K, SOMLYO AV, GOLDMAN YE, SOMLYO AP. (1989). Kinetics of contraction initiated by flash photolysis of caged adenosine triphosphate in tonic and phasic smooth muscles. *J Gen Physiol*; **94**(4):769-781.
50. HOROWITZ A, MENICE CB, LAPORTE R, MORGAN KG. (1996). Mechanisms of smooth muscle contraction. *Physiol Rev*; **76**(4):967-1003.
51. IIZUKA K, IKEBE M, SOMLYO AV, SOMLYO AP. (1994). Introduction of high molecular weight (IgG) proteins into receptor coupled, permeabilized smooth muscle. *Cell Calcium*; **16**(6):431-445.

52. ISHIDA K, PARE PD, THOMSON RJ, SCHELLENBERG RR. (1990). Increased in vitro responses of tracheal smooth muscle from hyperresponsive guinea pigs. *J Appl Physiol*; **68(4)**:1316-1320.
53. JACKSON AC, MURPHY MM, RASSULO J, CELLI BR, INGRAM RHJ. (2004). Deep breath reversal and exponential return of methacholine-induced obstruction in asthmatic and nonasthmatic subjects. *J Appl Physiol*; **96(1)**:137-142.
54. JAMES A, CARROLL N. (2000). Airway smooth muscle in health and disease; methods of measurement and relation to function. *Eur Respir J*; **15(4)**:782-789.
55. JEFFERY PK, WARDLAW AJ, NELSON FC, COLLINS JV, KAY AB. (1989). Bronchial biopsies in asthma. An ultrastructural, quantitative study and correlation with hyperreactivity. *Am Rev Respir Dis*; **140(6)**:1745-1753.
56. JIA Y, XU L, HEISLER S, MARTIN JG. (1995). Airways of a hyperresponsive rat strain show decreased relaxant responses to sodium nitroprusside. *Am J Physiol*; **269(1 Pt 1)**:L85-91.
57. JIANG H, RAO K, HALAYKO AJ, KEPRON W, STEPHENS NL. (1992). Bronchial smooth muscle mechanics of a canine model of allergic airway hyperresponsiveness. *J Appl Physiol*; **72(1)**:39-45.

58. JIANG H, RAO K, HALAYKO AJ, LIU X, STEPHENS NL. (1992). Ragweed sensitization-induced increase of myosin light chain kinase content in canine airway smooth muscle. *Am J Respir Cell Mol Biol*; **7(6)**:567-573.
59. JIANG H, RAO K, LIU X, HALAYKO AJ, LIU G, STEPHENS NL. (1994). Early changes in airway smooth muscle hyperresponsiveness. *Can J Physiol Pharmacol*; **72(11)**:1440-1447.
60. JONES R, STEUDEL W, WHITE S, JACOBSON M, LOW R. (1999). Microvessel precursor smooth muscle cells express head-inserted smooth muscle myosin heavy chain (SM-B) isoform in hyperoxic pulmonary hypertension. *Cell Tissue Res*; **295(3)**:453-465.
61. JUNIPER EF, FRITH PA, HARGREAVE FE. (1981). Airway responsiveness to histamine and methacholine: relationship to minimum treatment to control symptoms of asthma. *Thorax*; **36(8)**:575-579.
62. KAMM KE, STULL JT. (1985). Myosin phosphorylation, force, and maximal shortening velocity in neurally stimulated tracheal smooth muscle. *Am J Physiol*; **249(3 Pt 1)**:C238-47.
63. KANNAN MS, DANIEL EE. (1980). Structural and functional study of control of canine tracheal smooth muscle. *Am J Physiol*; **238(1)**:C27-33.
64. KELLEY CA, SELLERS JR, GOLDSMITH PK, ADELSTEIN RS. (1992). Smooth muscle myosin is composed of homodimeric heavy chains. *J Biol Chem*; **267(4)**:2127-2130.

65. KELLEY CA, TAKAHASHI M, YU JH, ADELSTEIN RS. (1993). An insert of seven amino acids confers functional differences between smooth muscle myosins from the intestines and vasculature. *J Biol Chem*; **268**(17):12848-12854.
66. KHROMOV A, SOMLYO AV, TRENTAM DR, ZIMMERMANN B, SOMLYO AP. (1995). The role of MgADP in force maintenance by dephosphorylated cross-bridges in smooth muscle: a flash photolysis study. *Biophys J*; **69**(6):2611-2622.
67. KHROMOV AS, WEBB MR, FERENCZI MA, TRENTAM DR, SOMLYO AP, SOMLYO AV. (2004). Myosin regulatory light chain phosphorylation and strain modulate adenosine diphosphate release from smooth muscle Myosin. *Biophys J*; **86**(4):2318-2328.
68. KNIGHT DA, STEWART GA, THOMPSON PJ. (1994). The respiratory epithelium and airway smooth muscle homeostasis: its relevance to asthma. *Clin Exp Allergy*; **24**(8):698-706.
69. KUO KH, WANG L, PARE PD, FORD LE, SEOW CY. (2001). Myosin thick filament lability induced by mechanical strain in airway smooth muscle. *J Appl Physiol*; **90**(5):1811-1816.
70. LAMBERT RK, WIGGS BR, KUWANO K, HOGG JC, PARE PD. (1993). Functional significance of increased airway smooth muscle in asthma and COPD. *J Appl Physiol*; **74**(6):2771-2781.

71. LAUZON AM, TRYBUS KM, WARSHAW DM. (1998). Molecular mechanics of two smooth muscle heavy meromyosin constructs that differ by an insert in the motor domain. *Acta Physiol Scand*; **164(4)**:357-361.
72. LAUZON AM, TYSKA MJ, ROVNER AS, FREYZON Y, WARSHAW DM, TRYBUS KM. (1998). A 7-amino-acid insert in the heavy chain nucleotide binding loop alters the kinetics of smooth muscle myosin in the laser trap. *J Muscle Res Cell Motil*; **19(8)**:825-837.
73. LEGUILLETTE R, GIL FR, ZITOUNI NB, LAJOIE-KADOCH S, SOBIESZEK A, LAUZON AM. (2005). (+)Insert Smooth Muscle Myosin Heavy Chain (SM-B) Isoform Expression in Human Tissues. *Am J Physiol Cell Physiol*;
74. LEGUILLETTE R, LAVIOLETTE M, LAUZON AM. (2005). Quantitative smooth muscle RNA analysis of asthmatic human bronchial biopsies. *Proc Am Thor Soc*; **2 (1)**:A338.
75. LIM TK, PRIDE NB, INGRAM RHJ. (1987). Effects of volume history during spontaneous and acutely induced air-flow obstruction in asthma. *Am Rev Respir Dis*; **135(3)**:591-596.
76. LOFGREN M, FAGHER K, WEDE OK, ARNER A. (2002). Decreased shortening velocity and altered myosin isoforms in guinea-pig hypertrophic intestinal smooth muscle. *J Physiol*; **544(Pt 3)**:707-714.

77. LOFGREN M, FAGHER K, WOODARD G, ARNER A. (2002). Effects of thyroxine on myosin isoform expression and mechanical properties in guinea-pig smooth muscle. *J Physiol*; **543(Pt 3)**:757-766.
78. LOS H, POSTMUS PE, BOOMSMA DI. (2001). Asthma genetics and intermediate phenotypes: a review from twin studies. *Twin Res*; **4(2)**:81-93.
79. LOUKIANOV E, LOUKIANOVA T, PERIASAMY M. (1997). Myosin heavy chain isoforms in smooth muscle. *Comp Biochem Physiol B Biochem Mol Biol*; **117(1)**:13-18.
80. LOW RB, MITCHELL J, WOODCOCK-MITCHELL J, ROVNER AS, WHITE SL. (1999). Smooth-muscle myosin heavy-chain SM-B isoform expression in developing and adult rat lung. *Am J Respir Cell Mol Biol*; **20(4)**:651-657.
81. MA X, CHENG Z, KONG H, et al. (2002). Changes in biophysical and biochemical properties of single bronchial smooth muscle cells from asthmatic subjects. *Am J Physiol Lung Cell Mol Physiol*; **283(6)**:L1181-9.
82. MACKLEM PT. (1996). A theoretical analysis of the effect of airway smooth muscle load on airway narrowing. *Am J Respir Crit Care Med*; **153(1)**:83-89.
83. MALMQVIST U, ARNER A. (1991). Correlation between isoform composition of the 17 kDa myosin light chain and maximal shortening velocity in smooth muscle. *Pflugers Arch*; **418(6)**:523-530.

84. MANNIKAROTTU AS, HYPOLITE JA, ZDERIC SA, WEIN AJ, CHACKO S, DISANTO ME. (2005). Regional alterations in the expression of smooth muscle myosin isoforms in response to partial bladder outlet obstruction. *J Urol*; **173**(1):302-308.
85. MCINTOSH JC, SIMECKA JW, ROSS SE, DAVIS JK, MILLER EJ, CASSELL GH. (1992). Infection-induced airway fibrosis in two rat strains with differential susceptibility. *Infect Immun*; **60**(7):2936-2942.
86. MITCHELL RW, ANTONISSEN LA, KEPRON W, KROEGER EA, STEPHENS NL. (1986). Effect of atropine on the hyperresponsiveness of ragweed-sensitized canine tracheal smooth muscle. *J Pharmacol Exp Ther*; **236**(3):803-809.
87. MITCHELL RW, NDUKWU IM, ARBETTER K, SOLWAY J, LEFF AR. (1993). Effect of airway inflammation on smooth muscle shortening and contractility in guinea pig trachealis. *Am J Physiol*; **265**(6 Pt 1):L549-54.
88. MITCHELL RW, RUHLMANN E, MAGNUSSEN H, LEFF AR, RABE KF. (1994). Passive sensitization of human bronchi augments smooth muscle shortening velocity and capacity. *Am J Physiol*; **267**(2 Pt 1):L218-22.
89. MORANO I, ERB G, SOGL B. (1993). Expression of myosin heavy and light chains changes during pregnancy in the rat uterus. *Pflugers Arch*; **423**(5-6):434-441.

90. MURPHY RA, HERLIHY JT, MEGERMAN J. (1974). Force-generating capacity and contractile protein content of arterial smooth muscle. *J Gen Physiol*; **64(6)**:691-705.
91. MURPHY RA, WALKER JS, STRAUSS JD. (1997). Myosin isoforms and functional diversity in vertebrate smooth muscle. *Comp Biochem Physiol B Biochem Mol Biol*; **117(1)**:51-60.
92. NATIONAL HEART L, AND BLOOD INSTITUTE. (1997). National Asthma Education Program Expert Panel Report II: Guidelines for the diagnosis and management of asthma. **NIH Publication No.:**97-4051A.
93. NIIMI A, MATSUMOTO H, TAKEMURA M, UEDA T, CHIN K, MISHIMA M. (2003). Relationship of airway wall thickness to airway sensitivity and airway reactivity in asthma. *Am J Respir Crit Care Med*; **168(8)**:983-988.
94. O'BYRNE PM, INMAN MD. (2003). Airway hyperresponsiveness. *Chest*; **123(3 Suppl)**:411S-416S.
95. PARE PD, ROBERTS CR, BAI TR, WIGGS BJ. (1997). The functional consequences of airway remodeling in asthma. *Monaldi Arch Chest Dis*; **52(6)**:589-596.
96. PATZAK A, PETZHOLD D, WRONSKI T, et al. (2005). Constriction velocities of renal afferent and efferent arterioles of mice are not related to SMB expression. *Kidney Int*; **68(6)**:2726-2734.

97. PRATUSEVICH VR, SEOW CY, FORD LE. (1995). Plasticity in canine airway smooth muscle. *J Gen Physiol*; **105(1)**:73-94.
98. RAO K, HE JA, HALAYKO AJ, PAN N, KEPRON W, STEPHENS NL. (1991). Increased ATPase activity and myosin light chain kinase (MLCK) content in airway smooth muscle from sensitized dogs. *Adv Exp Med Biol*; **304**:369-376.
99. ROVNER AS, FAGNANT PM, LOWEY S, TRYBUS KM. (2002). The carboxyl-terminal isoforms of smooth muscle myosin heavy chain determine thick filament assembly properties. *J Cell Biol*; **156(1)**:113-123.
100. ROVNER AS, FREYZON Y, TRYBUS KM. (1997). An insert in the motor domain determines the functional properties of expressed smooth muscle myosin isoforms. *J Muscle Res Cell Motil*; **18(1)**:103-110.
101. SCHELLENBERG RR, FOSTER A. (1984). In vitro responses of human asthmatic airway and pulmonary vascular smooth muscle. *Int Arch Allergy Appl Immunol*; **75(3)**:237-241.
102. SEOW CY, FREDBERG JJ. (2001). Historical perspective on airway smooth muscle: the saga of a frustrated cell. *J Appl Physiol*; **91(2)**:938-952.
103. SHERWOOD JJ, EDDINGER TJ. (2002). Shortening velocity and myosin heavy- and light-chain isoform mRNA in rabbit arterial smooth muscle cells. *Am J Physiol Cell Physiol*; **282(5)**:C1093-102.

104. SJUVE R, HAASE H, MORANO I, UVELIUS B, ARNER A. (1996). Contraction kinetics and myosin isoform composition in smooth muscle from hypertrophied rat urinary bladder. *J Cell Biochem*; **63(1)**:86-93.
105. SKLOOT G, PERMUTT S, TOGIAS A. (1995). Airway hyperresponsiveness in asthma: a problem of limited smooth muscle relaxation with inspiration. *J Clin Invest*; **96(5)**:2393-2403.
106. SOBIESZEK A, JERTSCHIN P. (1986). Urea-glycerol-acrylamide gel electrophoresis of acidic low molecular weight muscle proteins: rapid determination of myosin light chain phosphorylation in myosin, actomyosin, and whole muscle samples. *Electrophoresis*; **7**:417-425.
107. SOLWAY J. (2000). What makes the airways contract abnormally? Is it inflammation? *Am J Respir Crit Care Med*; **161(3 Pt 2)**:S164-7.
108. SOMLYO AP. (1993). Myosin isoforms in smooth muscle: how may they affect function and structure? *J Muscle Res Cell Motil*; **14(6)**:557-563.
109. SOMLYO AV, SOMLYO AP. (1968). Electromechanical and pharmacomechanical coupling in vascular smooth muscle. *J Pharmacol Exp Ther*; **159(1)**:129-145.
110. SPARROW MP, MOHAMMAD MA, ARNER A, HELLSTRAND P, RUEGG JC. (1988). Myosin composition and functional properties of smooth muscle from the uterus of pregnant and non-pregnant rats. *Pflugers Arch*; **412(6)**:624-633.

111. SPINA D. (1998). Epithelium smooth muscle regulation and interactions. *Am J Respir Crit Care Med*; **158**(5 Pt 3):S141-5.
112. (2005). Canadian Statistics -- Persons with asthma by age and sex.
113. STEPHENS NL. (2001). Airway smooth muscle. *Lung*; **179**(6):333-373.
114. STEPHENS NL, LI W, JIANG H, UNRUH H, MA X. (2003). The biophysics of asthmatic airway smooth muscle. *Respir Physiol Neurobiol*; **137**(2-3):125-140.
115. SWEENEY HL, ROSENFELD SS, BROWN F, et al. (1998). Kinetic tuning of myosin via a flexible loop adjacent to the nucleotide binding pocket. *J Biol Chem*; **273**(11):6262-6270.
116. SZYMANSKI PT, CHACKO TK, ROVNER AS, GOYAL RK. (1998). Differences in contractile protein content and isoforms in phasic and tonic smooth muscles. *Am J Physiol*; **275**(3 Pt 1):C684-92.
117. TAO FC, SHAH S, PRADHAN AA, TOLLOCZKO B, MARTIN JG. (2003). Enhanced calcium signaling to bradykinin in airway smooth muscle from hyperresponsive inbred rats. *Am J Physiol Lung Cell Mol Physiol*; **284**(1):L90-9.
118. TAO FC, TOLLOCZKO B, EIDELMAN DH, MARTIN JG. (1999). Enhanced Ca(2+) mobilization in airway smooth muscle contributes to airway hyperresponsiveness in an inbred strain of rat. *Am J Respir Crit Care Med*; **160**(2):446-453.

119. TAO FC, TOLLOCZKO B, MITCHELL CA, POWELL WS, MARTIN JG. (2000). Inositol (1,4,5)trisphosphate metabolism and enhanced calcium mobilization in airway smooth muscle of hyperresponsive rats. *Am J Respir Cell Mol Biol*; **23(4)**:514-520.
120. THOMSON NC. (1987). In vivo versus in vitro human airway responsiveness to different pharmacologic stimuli. *Am Rev Respir Dis*; **136(4 Pt 2)**:S58-62.
121. THOMSON RJ, BRAMLEY AM, SCHELLENBERG RR. (1996). Airway muscle stereology: implications for increased shortening in asthma. *Am J Respir Crit Care Med*; **154(3 Pt 1)**:749-757.
122. TUCK SA, MAGHNI K, POIRIER A, et al. (2004). Time course of airway mechanics of the (+)insert myosin isoform knockout mouse. *Am J Respir Cell Mol Biol*; **30(3)**:326-332.
123. VANBUREN P, WALLER GS, HARRIS DE, TRYBUS KM, WARSHAW DM, LOWEY S. (1994). The essential light chain is required for full force production by skeletal muscle myosin. *Proc Natl Acad Sci U S A*; **91(26)**:12403-12407.
124. VANBUREN P, WORK SS, WARSHAW DM. (1994). Enhanced force generation by smooth muscle myosin in vitro. *Proc Natl Acad Sci U S A*; **91(1)**:202-205.

125. WAGNER PD. (1981). Formation and characterization of myosin hybrids containing essential light chains and heavy chains from different muscle myosins. *J Biol Chem*; **256(5)**:2493-2498.
126. WANG CG, ALMIRALL JJ, DOLMAN CS, DANDURAND RJ, EIDELMAN DH. (1997). In vitro bronchial responsiveness in two highly inbred rat strains. *J Appl Physiol*; **82(5)**:1445-1452.
127. WANG L, PARE PD, SEOW CY. (2001). Selected contribution: effect of chronic passive length change on airway smooth muscle length-tension relationship. *J Appl Physiol*; **90(2)**:734-740.
128. WETZEL K, BALTATU O, NAFZ B, PERSSON PB, HAASE H, MORANO I. (2003). Expression of smooth muscle MyHC B in blood vessels of hypertrophied heart in experimentally hypertensive rats. *Am J Physiol Regul Integr Comp Physiol*; **284(2)**:R607-10.
129. WETZEL U, LUTSCH G, HAASE H, GANTEN U, MORANO I. (1998). Expression of smooth muscle myosin heavy chain B in cardiac vessels of normotensive and hypertensive rats. *Circ Res*; **83(2)**:204-209.
130. WHITE S, MARTIN AF, PERIASAMY M. (1993). Identification of a novel smooth muscle myosin heavy chain cDNA: isoform diversity in the S1 head region. *Am J Physiol*; **264(5 Pt 1)**:C1252-8.

131. WHITE SL, ZHOU MY, LOW RB, PERIASAMY M. (1998). Myosin heavy chain isoform expression in rat smooth muscle development. *Am J Physiol*; **275**(2 Pt 1):C581-9.
132. WOODCOCK-MITCHELL J, WHITE S, STIREWALT W, PERIASAMY M, MITCHELL J, LOW RB. (1993). Myosin isoform expression in developing and remodeling rat lung. *Am J Respir Cell Mol Biol*; **8**(6):617-625.
133. WOOLCOCK AJ, PEAT JK. (1989). Epidemiology of bronchial hyperresponsiveness. *Clin Rev Allergy*; **7**(3):245-256.
134. WOOLCOCK AJ, SALOME CM, YAN K. (1984). The shape of the dose-response curve to histamine in asthmatic and normal subjects. *Am Rev Respir Dis*; **130**(1):71-75.